CellPress

An activated form of NB-ARC protein RLS1 functions with cysteine-rich receptor-like protein RMC to trigger cell death in rice

Yiqin Wang[1,6], Zhenfeng Teng[1,6], Hua Li[1,6], Wei Wang[1], Fan Xu[1], Kai Sun[1], Jinfang Chu[2], Yangwen Qian[3], Gary J. Loake[4], Chengcai Chu[1,5,*] and Jiuyou Tang[1,*]

[1]State Key Laboratory of Plant Genomics, Institute of Genetics and Developmental Biology, the Innovative Academy of Seed Design, Chinese Academy of Sciences, Beijing 100101, China

[2]Institute of Genetics and Developmental Biology and National Center for Plant Gene Research (Beijing), Chinese Academy of Sciences, Beijing 100101, China

[3]Biogle Genome Editing Center, Changzhou 213125, China

[4]Institute of Molecular Plant Sciences, School of Biological Sciences, University of Edinburgh, Edinburgh EH9 3BF, UK

[5]Guangdong Laboratory for Lingnan Modern Agriculture, State Key Laboratory for Conservation and Utilization of Subtropical Agro-Bioresources, College of Agriculture, South China Agricultural University, Guangzhou 510642, China

[6]These authors contributed equally to this article.

*Correspondence: Chengcai Chu (ccchu@genetics.ac.cn), Jiuyou Tang (jytang@genetics.ac.cn)

https://doi.org/10.1016/j.xplc.2022.100459

ABSTRACT

A key event that follows pathogen recognition by a resistance (R) protein containing an NB-ARC (nucleotide-binding adaptor shared by Apaf-1, R proteins, and Ced-4) domain is hypersensitive response (HR)-type cell death accompanied by accumulation of reactive oxygen species and nitric oxide. However, the integral mechanisms that underlie this process remain relatively opaque. Here, we show that a gain-of-function mutation in the NB-ARC protein RLS1 (Rapid Leaf Senescence 1) triggers high-light-dependent HR-like cell death in rice. The *RLS1*-mediated defense response is largely independent of salicylic acid accumulation, NPR1 (Nonexpressor of Pathogenesis-Related Gene 1) activity, and RAR1 (Required for *Mla12* Resistance 1) function. A screen for suppressors of *RLS1* activation identified *RMC* (Root Meander Curling) as essential for the *RLS1*-activated defense response. *RMC* encodes a cysteine-rich receptor-like secreted protein (CRRSP) and functions as an RLS1-binding partner. Intriguingly, their co-expression resulted in a change in the pattern of subcellular localization and was sufficient to trigger cell death accompanied by a decrease in the activity of the antioxidant enzyme APX1. Collectively, our findings reveal an NB-ARC–CRRSP signaling module that modulates oxidative state, the cell death process, and associated immunity responses in rice.

Key words: hypersensitive response, NB-ARC protein, cysteine-rich receptor-like secreted protein, disease resistance, antioxidant enzymes

INTRODUCTION

Plant immunity is largely underpinned by a molecular surveillance system that detects the presence of potential pathogens (Mantelin et al., 2011). In this context, perception of diverse pathogen-associated molecular patterns (PAMPs) by plasma membrane (PM)-resident pattern recognition receptors results in PAMP-triggered immunity (PTI) (Chisholm et al., 2006). To suppress PTI and colonize the host, phytopathogens have evolved a plethora of effector proteins that are

typically delivered to the inside of plant cells, disabling defense responses and reprograming plant physiology to aid pathogenesis (da Cunha et al., 2007). In response, plants have evolved a repertoire of resistance (R) proteins to detect either directly or, routinely, indirectly the presence of pathogen effector proteins, resulting in the deployment of a phalanx of

plant defense responses. This effector-triggered immunity (ETI) provides effective protection against attempted microbial ingress (Gassmann and Bhattacharjee, 2012).

A common feature of major R proteins is the presence of both a nucleotide-binding site (NBS) and leucine-rich repeat (LRR) domains (Urbach and Ausubel, 2017). The NB domain is also a conserved region shared by Apaf-1 and Ced-4 proteins, which play critical roles in the regulation of programmed cell death in animal cells (Inohara and Nunez, 2001). In this context, this motif is known as the NB-ARC (nucleotide-binding, Apaf-1, R proteins, and Ced-4) or NOD (nucleotide oligomerization domain) (Hamada et al., 2013). The universal prevalence of such a domain implies an evolutionary conservation of cell death effectors between animals and plants (van der Biezen and Jones, 1998; Jiao et al., 2012). In general, the function of R proteins is tightly controlled by a series of regulators that maintain an auto-inhibited state in the absence of pathogens (Tang et al., 2019). Nevertheless, some reports have shown that mutations in NB-ARC proteins are sufficient to result in pathogen-independent defense activation. For example, gain-of-function mutations in SSI4 (Suppressor of *npr1*-5-Based SA Insensitivity 4), SNC1 (Suppressor of *npr1-1*, Constitutive 1), SLH1 (Sensitive to Low Humidity 1), UNI (U-NI, like sea urchin), and NLS1 (Necrotic Leaf Sheath 1) all lead to constitutive defense responses in plants (Shirano et al., 2002; Zhang et al., 2003; Noutoshi et al., 2005; Igari et al., 2008; Tang et al., 2011).

R protein-triggered defense responses are closely associated with the development of the hypersensitive response (HR), a localized programmed execution of plant cells at the site of attempted microbial infection, which is thought to help restrict pathogen growth (Greenberg and Yao, 2004). This pathogen-triggered cell death process in plants has common regulatory and mechanistic features with apoptosis in animals (La Camera et al., 2005; Balint-Kurti, 2019). One of the earliest events in the pathogen–host interaction is the rapid production of reactive oxygen species (ROS), including singlet oxygen ($^1O_2$), superoxide radical (O_2^-), hydrogen peroxide (H_2O_2), and so on, termed the oxidative burst (Grant and Loake, 2000), which is also important for cell death development (Greenberg and Yao, 2004; Wang et al., 2013a). In parallel to ROS production is the pathogen-triggered nitrosative burst, resulting in the generation of nitric oxide (NO) and associated reactive nitrogen species (RNS) (Wendehenne et al., 2004; Astier et al., 2011; Yu et al., 2014; Lindermayr and Durner, 2015). NO bioactivity is principally mediated by S-nitrosylation, the addition of a NO moiety to a rare, highly reactive cysteine thiol to form an S-nitrosothiol (SNO) (Wang et al., 2009; Astier et al., 2011; Yun et al., 2011; Lindermayr, 2018). Significantly, NO function is thought to be closely interconnected with that of ROS during cell death development (Delledonne et al., 1998, 2001); the reaction of NO with superoxide anion (O_2^-) results in the formation of peroxynitrite ($ONOO^-$) in plants, which may play a role in protein or lipid nitration and DNA damage (Izbianska et al., 2018; Lv et al., 2022). Many abiotic conditions, including high light (HL) and salt stress, have also been linked with the initiation of cell death. HL levels can create an overflow of electrons from the photosynthetic electron transport system in chloroplasts, which results in the generation of ROS (Hideg et al., 2006; Caverzan et al., 2014). Thus, HL levels have been associated with cell death formation, especially in the absence of key antioxidant mechanisms (Kliebenstein et al., 1999; Vranova et al., 2002). Collectively, the accumulating data suggest significant crosstalk between HL, RNS, and ROS during cell death generation (Wang et al., 2013a), although the molecular basis of these interactions is still not well understood.

Receptor-like protein kinases, which contain extracellular receptor and cytoplasmic catalytic kinase domains, and receptor-like proteins are associated with both PTI and ETI (Mantelin et al., 2011). These proteins are classified into subfamilies according to the composition of their extracellular domains (Shiu and Bleecker, 2001). Cysteine-rich receptor-like kinases (CRKs), also termed Domain of Unknown Function 26 (DUF26; Gnk2 or stress-antifungal domain; PF01657) proteins, possess an extracellular domain harboring a conserved cysteine motif (C-8X-C-2X-C) and form a subfamily of receptor-like protein kinases with more than 40 members in *Arabidopsis* and rice (Wrzaczek et al., 2010; Chern et al., 2016). *CRK* expression is induced by ozone (O_3), salicylic acid (SA), or PAMPs (Wrzaczek et al., 2010). Overexpression of the CRK members CRK5, CRK13, CRK28, or CRK36 in *Arabidopsis* led to enhanced resistance to *Pseudomonas syringae* pv. *tomato* (*Pst*) DC3000 and HR-like cell death (Chen et al., 2003, 2004; Acharya et al., 2007; Lee et al., 2017; Yadeta et al., 2017). Recently, CRK2 has been shown to associate with and activate RESPIRATORY BURST OXIDASE HOMOLOG D to trigger MAMP-induced ROS production, revealing a mechanism by which a CRK regulates the oxidative burst (Kimura et al., 2020).

With homology to the extracellular domain of CRKs, cysteine-rich receptor-like secreted proteins (CRRSPs), which lack the kinase domain, contain one or two DUF26 motifs. One of the best characterized CRRSPs is Gnk2 from *Gingko biloba* with a single DUF26 (sdCRRSP), which acts as a mannose binding lectin *in vitro* with antifungal activity (Miyakawa et al., 2009). The other two are AFP1 and AFP2, which show antifungal activity in maize that can be blocked by the repetitive effector Rsp3 of the biotrophic fungus *Ustilago maydis* (Ma et al., 2018). Bioinformatics analysis has established that rice, as well as the *Brassicaceae*, displays lineage-specific evolution with a large number of CRRSPs with two DUF26 motifs (ddCRRSPs) and the absence of sdCRRSPs (Vaattovaara et al., 2019). Although insights into the function of CRKs are emerging (Chen et al., 2003, 2004; Acharya et al., 2007; Lee et al., 2017), a potential role for CRRSPs in plant immunity and associated HR cell death remains to be established (Miyakawa et al., 2009).

Here, we identified and characterized the (S)NO over-accumulation mutant *noe2* (*nitric oxide excess2*). *NOE2* encodes the NB-ARC protein Rapid Leaf Senescence 1 (RLS1), which in its activated form works with a ddCRRSP, resulting in rapid activation of HR-like cell death in rice, accompanied by suppression of the antioxidant system.

RESULTS

Identification and characterization of the *noe2* mutant

We previously screened a series of mutants with increased SNO content, including the reported *noe1* with a loss-of-function
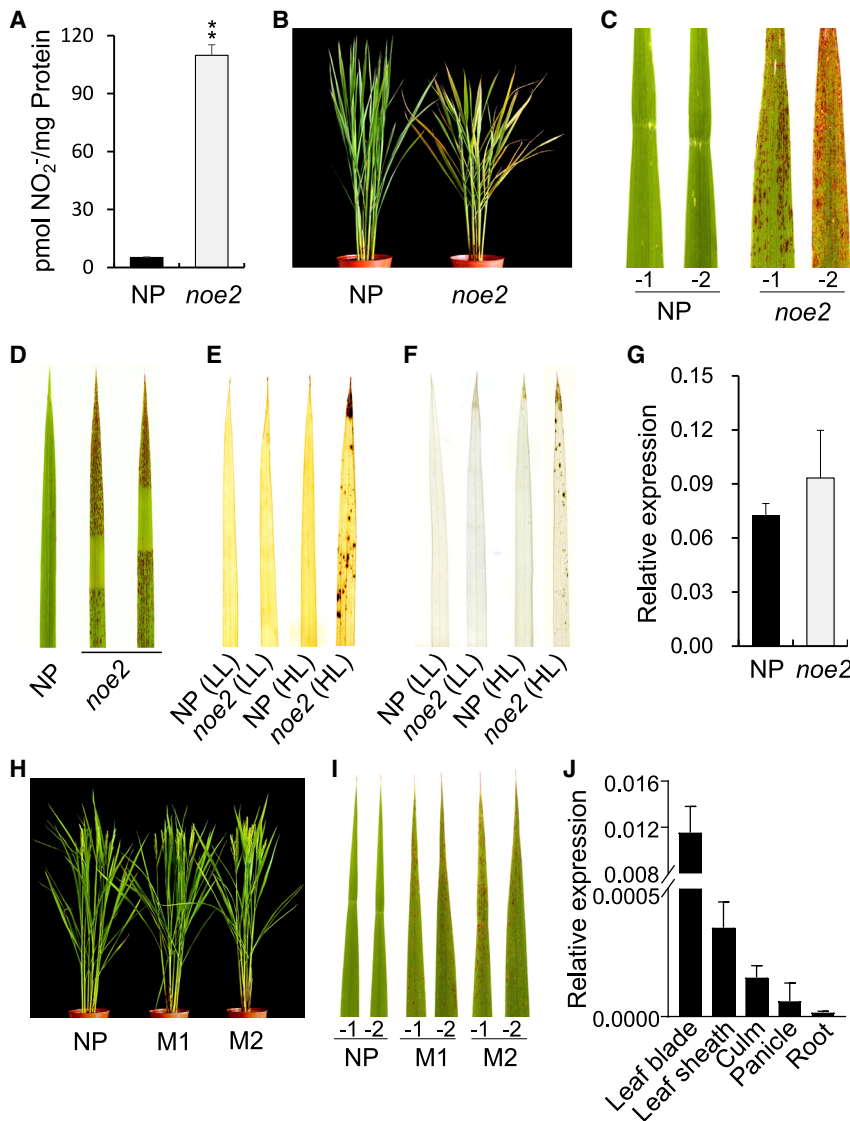
Figure 1. Characterization of *noe2* and its target gene *LOC_Os02g10900*.

(A) SNO content of *noe2* and wild-type Nipponbare (NP) demonstrated by the result of a Saville-Griess assay using leaves of 45-day-old seedlings grown in the field. Values are the means ± SD ($n = 3$).

(B and C) HR-like leaf cell death phenotype of the *noe2* whole plant **(B)** and the first ("−1") and second ("−2") fully expanded leaves from top to bottom **(C)**, which exhibited yellow-brown lesions.

(D) Leaf area of *noe2* shielded from high light (HL) under natural field conditions (light intensity ∼1600 µmol m^{-2} s^{-1}) did not develop HR-like cell death.

(E and F) 3,3-Diaminobenzidine (DAB) staining **(E)** and trypan blue (TB) staining **(F)** indicated the accumulation of H_2O_2 and cell death, respectively, induced by HL treatment of 2-week-old rice seedlings grown in a greenhouse under low light (LL, light intensity ∼400 µmol m^{-2} s^{-1}) conditions.

(G) Expression level of *LOC_Os02g10900* in the leaves of 45-day-old *noe2* seedlings grown in the field compared with the wild-type control. Values are the means ± SD ($n = 3$).

(H and I) Transgenic reconstitution experiment in which mutated (M) *LOC_Os02g10900* was over-expressed in wild-type NP plants. Two representative independent transgenic lines termed M1 and M2 are shown. HR-like leaf cell death lesions can be observed in whole plants **(H)** and the first ("−1") and second ("−2") fully expanded leaves from top to bottom **(I)** in transgenic lines.

(J) Expression patterns of *LOC_Os02g10900* in different tissues of rice revealed by qRT–PCR analysis. Values are the means ± SD ($n = 3$). All experiments were repeated three times with similar results. **Indicates a significant difference according to Student's *t*-test ($P < 0.01$).

mutation in *Catalase-C* (*CAT-C/NOE1*) (Lin et al., 2012). Here, we report another NO-excess mutant, *noe2*, which exhibits a lesion mimic, leaf cell death phenotype (Figure 1A–1C). Similar to *noe1*, a higher SNO content was associated with higher H_2O_2 levels in *noe2* (Supplemental Figure 1A and 1B). However, the leaf cell death phenotype of *noe2* was different from that of *noe1* (Supplemental Figure 1C). In *noe1*, H_2O_2 accumulated in response to HL levels owing to a reduction in leaf catalase activity to ∼70% that of wild-type Nipponbare (NP) plants. Subsequently, leaves initially exhibited a bleached phenotype, followed by necrosis (Supplemental Figure 1C) (Lin et al., 2012). By contrast, cell death in *noe2* plants was spatially restricted, resembling HR cell death (Figure 1B and 1C; Supplemental Figure 1C). To further explore these cell death phenotypes, we generated the *noe1 noe2* double mutant. Significantly, *noe1 noe2* plants exhibited a superimposed cell death phenotype with features of both *noe1* and *noe2* (Supplemental Figure 1C). Collectively, these data suggest that the cell death phenotypes of *noe1* and *noe2* plants are not mediated by the same genetic pathway.

In *noe2* plants, the HR-like leaf cell death phenotype commenced at the seedling stage. Once new leaves had fully expanded in the field under natural growth conditions (high light, HL; light intensity ∼1600 µmol m^{-2} s^{-1}), HR-like lesions initiated from the leaf tip and gradually developed over the entire leaf (Figure 1B and 1C). Similar HR-like lesions were also observed on the culm and sheath (Supplemental Figure 1D). Furthermore, the HR-like cell death phenotype of *noe2* plants was affected by HL, as no HR-like lesions were found in shielded leaf areas (Figure 1D). Similarly, there were no lesions on leaves of *noe2* seedlings grown in the greenhouse under low light conditions (low light [LL]; light intensity ∼400 µmol m^{-2} s^{-1}). However, when 2-week-old LL-grown *noe2* plants were transferred to HL, rapid HR-like leaf cell death began to appear. In the greenhouse, HL treatment (light intensity ∼800 µmol m^{-2} s^{-1}) also triggered HR-like cell death in *noe2* plants, accompanied by H_2O_2 accumulation (Figure 1E and 1F). In aggregate, these findings imply that the observed HR-like cell death phenotype in *noe2* plants is dependent on HL.

As *noe2* was identified by virtue of its elevated SNO content, the role of NO in the HR-like cell death phenotype was

analyzed. Two-week-old LL-grown *noe2* seedlings were treated with different concentrations of the NO donor sodium nitroprusside. However, no HR-like leaf cell death phenotype was observed following up to 50 mM SNP treatment (data not shown), which suggests that a higher SNO content alone may not be sufficient to activate the HR-like cell death in *noe2* plants, although elevated SNO levels may contribute to the development of HR-like cell death in *noe2* plants.

Map-based cloning of *NOE2*

Although *noe2 was* identified from a T-DNA insertion population, the SNO over-accumulation and associated HR-like cell death phenotype of *noe2* plants did not co-segregate with the T-DNA insertion. Thus, a *noe2* line without the T-DNA insertion was isolated by backcrossing to the wild type. An F_2 mapping population was established using a cross between *noe2* (*japonica*) and Minghui 63 (*indica*), from which 306 individual plants exhibiting the *noe2* mutant phenotype were collected. Through map-based cloning, the mutation site was delimited to chromosome 2 between genetic markers 5.65M and 5.82M (Supplemental Figure 1E). After sequencing all 29 candidate genes within this region, only one T-to-C transition was found at nucleotide position 1097 in the coding sequence of *LOC_Os02g10900*, which resulted in an amino acid (aa) substitution at position 366 from Val (GTT) to Ala (GCT) in *noe2* plants. There was no significant difference in *LOC_Os02g10900* transcript level between *noe2* and wild-type NP plants (Figure 1G), suggesting no transcriptional activation of this gene in *noe2* plants. To confirm that *LOC_Os02g10900* possessed the *noe2* function, the Ala366 version of this gene was overexpressed in wild-type plants, and all eight independent positive T_0 transformants showed a *noe2*-like leaf cell death phenotype (Figure 1H and 1I). Therefore, this transgenic reconstitution experiment confirmed that *NOE2* is *LOC_Os02g10900*.

LOC_Os02g10900 has previously been named *Rapid Leaf Senescence 1* (*RLS1*) in rice and may be involved in chloroplast degradation during rice leaf senescence (Jiao et al., 2012). To avoid confusion, *NOE2* is hereafter unified into *RLS1*. *RLS1* encodes a 1040-aa protein containing a coiled-coil (CC) region, an NB-ARC domain at the N terminus, and three armadillo (ARM) motifs at the C terminus; it is ubiquitously expressed in different rice tissues (Figure 1J and Supplemental Figure 1F). It shares high sequence similarity in the NB-ARC domain with characterized rice R proteins, especially in the kinase, GLPL, RNBS-D, and MHDV motifs (Supplemental Figure 2A and 2B). The CC region from 65 to 91 aa of RLS1 is conserved in reported NLR proteins that contain a typical CC motif (Supplemental Figure 2C–2E). The NB-ARC domain is a conserved signaling motif shared by plant R proteins and regulators of apoptosis in animals, the activation of which results in cell death (van der Biezen and Jones, 1998; Tameling et al., 2006; Takken and Tameling, 2009; Elmore et al., 2011). The ARM motif, containing 38–45 aa residues, has been implicated in mediating protein–protein interactions (Supplemental Figure 1F) (Tewari et al., 2010). In the *rls1* mutant, a single C-to-T nucleotide substitution resulted in a Ser (TCT) to Phe (TTT) change at aa 994 in the C terminus of RLS1 (Jiao et al., 2012).

### *noe2* is an incompletely dominant gain-of-function mutant

The F_1 generation of *noe2* crossed with the wild type showed a *noe2*-like phenotype but with a change in lesion appearance: more yellow- than brown-based lesions relative to *noe2* plants (Figure 2A), indicating that *noe2* is an incompletely dominant mutation. We subsequently refer to the mutated *RLS1* in *noe2* as *RLS1-D*.

RNAi-mediated repression of *RLS1-D* expression in independent *noe2* plants recovered a wild-type leaf phenotype with no cell death. By contrast, repression of *RLS1* expression in wild-type plants had no impact on leaf phenotype (Figure 2B). The cell death phenotype could be suppressed by overexpression of *RLS1* in *noe2* (Figure 2C), whereas overexpression of *RLS1-D* in wild-type plants caused the appearance of HR-like leaf cell death (Figure 1H and 1I). Collectively, these results suggested that *noe2* is a gain-of-function mutation and the formation of *noe2*-dependent HR-like leaf cell death correlates with the amount of *RLS1-D* transcripts, implying a dose-dependent effect of *RLS1-D* in mediating HR-like cell death.

RLS1-D-mediated disease resistance is independent of SA accumulation and signaling

To investigate the possible role of RLS1 in disease resistance, *noe2* plants were challenged with the bacterial blight pathogen *Xanthomonas oryzae* pv. *oryzae* (*Xoo*) strain T7174 race 1 (T1). The *noe2* plants showed a significantly higher resistance level to bacterial blight than the wild-type plants (Figure 2D and 2E). Furthermore, the extent of pathogen resistance appeared to correlate with the level of *RLS1-D* expression, as F_1 heterozygous plants showed a resistance level intermediate between that of wild-type and *noe2* plants (Figure 2D and 2E). Repressing the expression of *RLS1* in wild-type plants did not significantly change the level of resistance against *Xoo* strain T1. Moreover, repressing the expression of *RLS1-D* in *noe2* plants significantly decreased the resistance level of the corresponding transgenic plants and resulted in no leaf cell death phenotype (Figure 2B and 2F). Overexpression of *RLS1* in *noe2* resulted in a loss of the HR-like leaf cell death phenotype and a reduced disease resistance level (Figure 2G). Consistent with these results, overexpression of *RLS1-D* in wild-type plants also significantly increased the resistance level of the resulting transgenic plants (Figure 2H). Therefore, the expression of *RLS1-D* transcripts led to the activation of disease resistance in *noe2* plants, which also resulted in an increase in H_2O_2 content (Figure 2I).

During HR, the level of SA, an essential component of the defense response network in plants, is known to increase with concomitant activation of SA-dependent defense responses, such as *Pathogenesis-Related* (*PR*) genes (Gaffney et al., 1993; Durrant and Dong, 2004). To examine whether the disease resistance and HR-like cell death phenotype of *noe2* were dependent upon SA accumulation, the content of SA in *noe2* plants was determined. The free SA content in 60-day-old *noe2* plants was approximately two times higher than that of the wild-type controls (Supplemental Figure 3A). Furthermore, markers of defense responses, *PR1b*, *PR2*, *PR5*, and *PR10*, were also upregulated in *noe2* plants (Supplemental Figure 3B–3E). To determine the potential role of SA in *RLS1-D*-triggered defense responses,
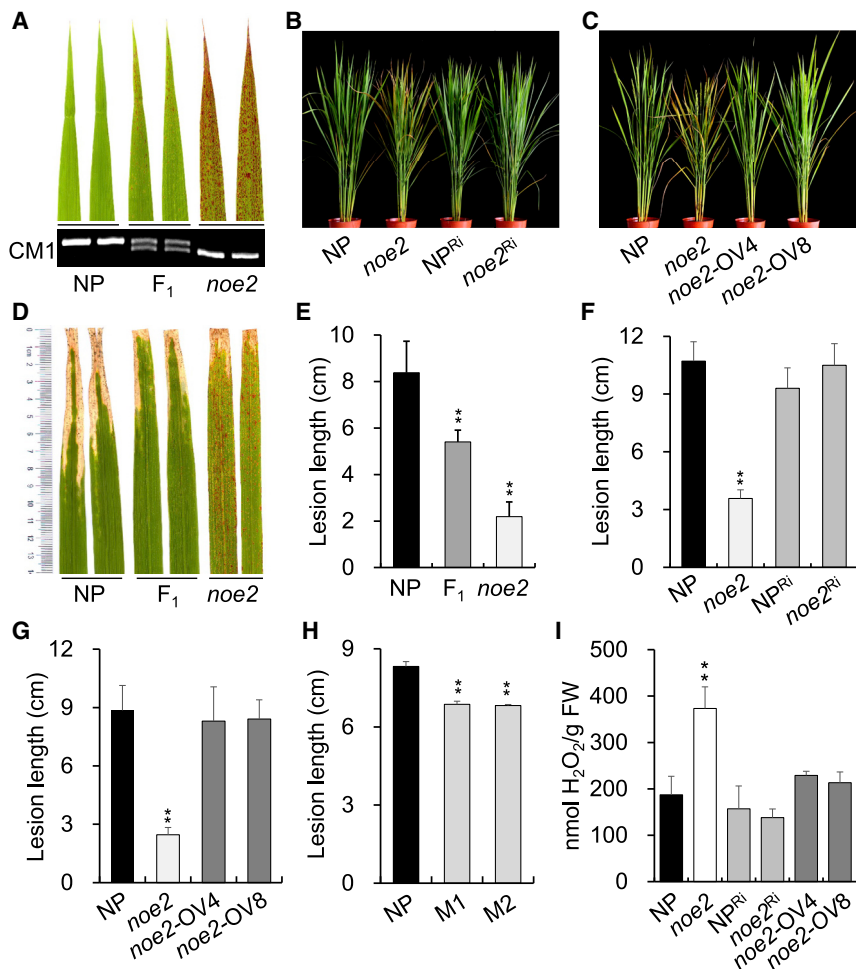
Figure 2. *noe2* is a gain-of-function mutant.

(A) *noe2*-like cell death phenotype shown on the leaves of F_1 plants obtained from a cross between *noe2* and wild-type NP. CM1, a derived cleaved amplified polymorphism sequences (dCAPS) marker, which demonstrated the fragment difference of heterozygous F_1 with *noe2* and the wild-type control.

(B and C) Both *RLS1* RNAi (*noe2*^Ri^) **(B)** and *RLS1* overexpression (*noe2*-OV4 and *noe2*-OV8) **(C)** could revert the HR-like leaf cell death phenotype of *noe2* to wild type.

(D and E) Disease phenotypes **(D)** and lesion lengths **(E)** of wild-type, *noe2*, and their F_1 plants were recorded at 14 days after inoculation (dai) with the bacterial blight pathogen *Xanthomonas oryzae* pv. *oryzae* (*Xoo*) strain T7174 (T1).

(F and G) Bacterial blight lesion lengths of *RLS1-D* RNAi **(F)** and *RLS1* overexpression **(G)** plants in the *noe2* background 14 dai with the bacterial blight pathogen *Xoo* strain T1.

(H) Bacterial blight lesion length of *RLS1-D* over-expression plants in the wild-type background 14 dai with the bacterial blight pathogen *Xoo* strain T1.

(I) Changes in H_2O_2 content in leaves of the indicated plant lines. When the lesions first appeared in *noe2*, leaves of the same developmental age grown under normal field conditions were harvested at the booting stage. Values are the means ± SD of 3 biological replications (8–10 leaves per replication) in **(E–I)**. All experiments were repeated three times with similar results. **Indicates a significant difference according to Student's *t*-test ($P < 0.01$).

NahG, a bacterial gene encoding salicylate hydroxylase that converts SA into catechol, was expressed in wild-type and *noe2* plants (Figure 3A–3C). Significantly, the expression of *NahG* reduced SA levels in the corresponding transgenic plants (Figure 3D). In the absence of pathogen challenge, overexpression of *NahG* in wild-type plants resulted in the formation of leaf lesions, mainly located at the old leaf tip area, as described previously (Heck et al., 2003; Tang et al., 2011). Overexpression of *NahG* had no negative effect on the formation of HR-like cell death in the *noe2* mutant (Figure 3B). Consistently, the increased expression of *PR1b*, *PR2*, *PR5*, and *PR10* in *noe2* was not alleviated or was even reinforced by *NahG* expression (Supplemental Figure 3B–3E). When wild-type and *noe2 plants were* infected with *Xoo* strain T1, the expression of *NahG* led to a significant reduction in disease resistance in both materials. The significant disruption of *noe2*-triggered disease resistance to T1 in *noe2 NahG* suggests a certain degree of interaction between *NahG* expression and *noe2* mutation. However, the resistance level of *noe2 NahG* plants was still greater than that of *NahG* plants (Figure 3E), implying that *noe2* also triggered SA-independent defense responses, resulting in constitutive cell death.

The expression level of *Nonexpressor of Pathogenesis-Related Genes 1* (*NPR1*), the master regulator of SA-dependent responses (Dong, 2004), was upregulated in *noe2* and downregulated by *NahG* overexpression (Supplemental Figure 3F). To explore this further, we generated a *noe2* double mutant with *npr1* (Figure 3F–3H). *Required for Mla12 Resistance 1* (*RAR1*) is one of the few identified downstream components that have been shown to play an important role in regulating the stability of multiple NLR proteins (Holt et al., 2005). We also generated a *rar1 noe2* double mutant to examine the role of RAR1 in *RLS1-D*-mediated leaf cell death. Both *noe2 npr1* and *noe2 rar1* double mutants exhibited an indistinguishable HR-like leaf cell death phenotype similar to that of *noe2* plants (Figure 3G–3I). Furthermore, when infected with *Xoo* strain T1, both *noe2 npr1* and *noe2 rar1* still showed increased resistance compared with that of the *npr1* and *rar1* single mutants (Figure 3J). Therefore, the resistance established by *RLS1-D* does not appear to be dependent upon either *NPR1* or *RAR1* function.

Identification and characterization of a *noe2* suppressor mutant

To further reveal the molecular mechanism underpinning *RLS1-D* function in the development of HR-like cell death, we carried out a genetic suppressor screen. From the resulting mutant population, one line with complete abolition of the leaf lesion phenotype was identified and termed *noe2 cell death suppressor 1* (*ncs1*). Except for the abolition of the HR-like cell death phenotype, *noe2 ncs1* plants did not show any other phenotypic alterations
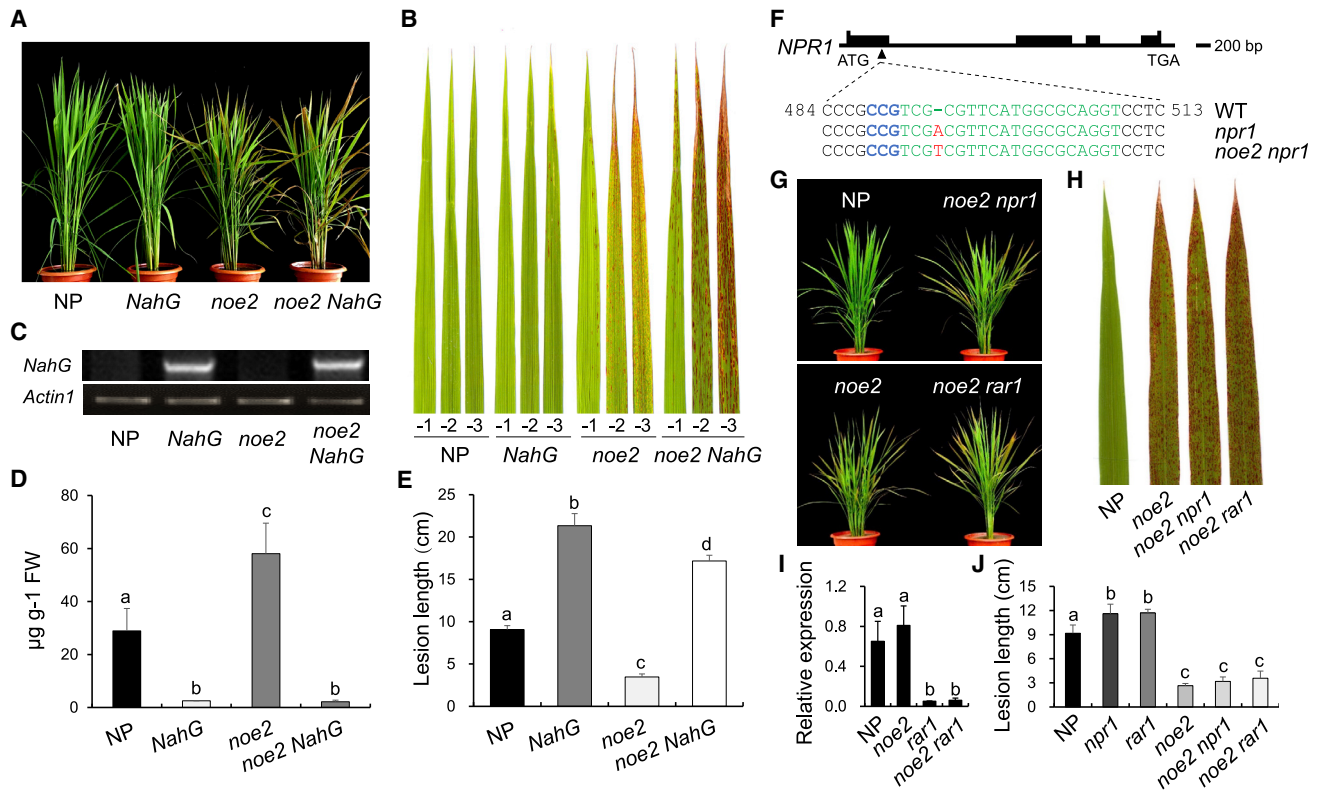
Figure 3. *RLS1-D*-triggered cell death is independent of SA accumulation, NPR1, and RAR1.
(A) Phenotypes of transgenic plants obtained by overexpressing *NahG* in wild-type and *noe2* plants.
(B) HR-like leaf cell death phenotype after *NahG* transgene expression in *noe2* or wild-type plants. "−1", "−2", and "−3" indicate the first, second, and third leaves from top to bottom.
(C) RT–PCR results show the overexpression of *NahG* in *noe2* or wild-type background plants.
(D) Total SA content in *NahG*-overexpressing transgenic plants in the wild-type or *noe2* background. Values are the means ± SD (*n* = 3).
(E) Disease resistance of *NahG*-overexpressing transgenic plants in the wild-type or *noe2* background to the bacterial blight pathogen *Xoo* strain T1. Lesion length was recorded at 14 dai.
(F) Sequence analysis of *npr1* and *noe2 npr1* plants to confirm loss of function of the target gene *NPR1*.
(G) Whole-plant phenotypes of the *noe2 npr1* and *noe2 rar1* double mutants.
(H) HR-like leaf cell death phenotypes in the *noe2 npr1* and *noe2 rar1* double mutants, which suggest that cell death of *noe2* is independent of *NPR1* and *RAR1*.
(I) Expression levels of *RAR1* in *rar1* and the *noe2 rar1* double mutant confirm the successful silencing of *RAR1*. Values are the means ± SD (*n* = 3).
(J) Disease resistance of the indicated lines to the bacterial blight pathogen *Xoo* strain T1. Lesion length was recorded at 14 dai. Both *noe2 npr1* and *noe2 rar1* double mutants showed increased disease resistance compared with the *npr1* or *rar1* single mutant. Values are the means ± SD of 3 biological replications (8–10 leaves per replication) in **(E–J)**. All experiments were repeated three times with similar results. Letters above bars indicate statistically different groups using a one-way ANOVA, followed by Duncan's multiple range test (*P* < 0.05). See also Supplemental Figure 3 and Supplemental Table 1.

compared with *noe2* plants (Figure 4A). Map-based cloning revealed that the *ncs1* mutation resided in *LOC_Os04g56430*, which encoded a CRRSP with two DUF26 domains (ddCRRSP) (Supplemental Figure 4A). This gene was previously reported as *Oryza sativa Root Meander Curling* (*OsRMC*) and implicated in jasmonate (JA) responses and salt resistance (Jiang et al., 2007; Zhang et al., 2009; Serra et al., 2013). Thus, we subsequently refer to this CRRSP as RMC.

Sequence analysis revealed a 26-bp deletion before the ATG start codon of *RMC* in the *ncs1* mutant, which resulted in a loss of protein function and elimination of leaf cell death (Figure 4B). To confirm that *RMC* was *NCS1*, we first performed a complementation test by overexpressing *RMC* in *noe2 ncs1* plants. In a total of six *RMC*-overexpressing transgenic lines in the *noe2 ncs1* background (*ncs1-C1/C2*), the *noe2* HR-like leaf

cell death phenotype was re-established (Figure 4C). We also obtained two independent lines harboring a mutation in *RMC* generated by the CRISPR-Cas9 knockout system in the *noe2* background, which we termed *noe2 ncs1-cr1* and *noe2 ncs1-cr2*. Sequence analysis showed that both knockout lines had an adenine (A) insertion at the 29 bp position after the start codon, resulting in a frame-shift mutation (Figure 4B). As expected, both lines showed a phenotype similar to that of *noe2 ncs1* plants, that is, a suppression of the HR-like leaf cell death phenotype and failure of RMC protein accumulation (Figure 4D and 4E). Collectively, these findings suggest that *RMC* and *NCS1* are the same gene.

Consistent with the leaf phenotype, *noe2 ncs1* and the knockout lines *noe2 ncs1-cr1* and *noe2 ncs1-cr2* showed lower H_2O_2 content compared with *noe2* plants, whereas the complemented lines *ncs1-C1* and *ncs1-C2* exhibited a higher H_2O_2 content
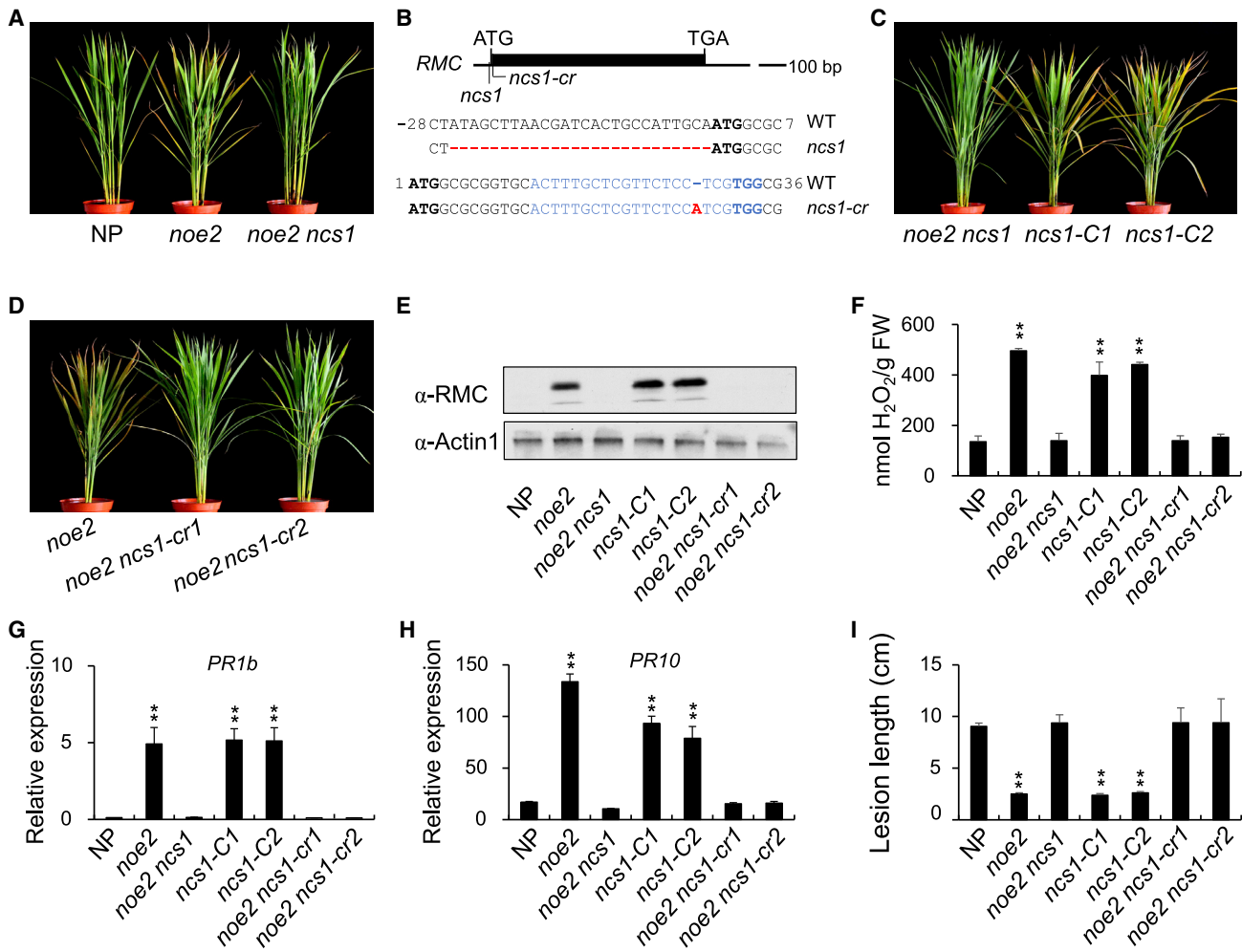
Figure 4. *RMC* is indispensable for *noe2*-triggered HR-like leaf cell death.
(A) Morphology of the *noe2 ncs1* double mutant compared with *noe2* and the wild type.
(B) *RMC* genomic sequence analysis of *ncs1* and CRISPR-Cas9-modified plants (*ncs1-cr*) in the *noe2* genetic background. WT, non-mutated *RMC* gene.
(C) Morphology of RMC overexpression lines in the *noe2 ncs1* background, *ncs1-C1* and *ncs1-C2*, compared with *noe2 ncs1*.
(D) Morphology of RMC knockout lines in the *noe2 ncs1* background, *noe2 ncs1-cr1* and *noe2 ncs1-cr2*, compared with *noe2*.
(E) Protein level of RMC in shoots of the indicated plant lines. Immunoblotting was performed with the Actin antibody as a loading control, and the level of RMC was detected by anti-RMC antibody.
(F–H) Changes in H_2O_2 content **(F)** and *PR1b* **(G)** and *PR10* **(H)** gene expression in leaves of the indicated plant lines. When the lesions first appeared in *noe2*, leaves of the same developmental age grown under normal field conditions were harvested at the booting stage. Values are the means ± SD ($n = 3$).
(I) Bacterial blight lesion lengths of indicated lines 14 days after inoculation with the bacterial blight pathogen *Xoo* strain T1. Values are the means ± SD of 3 biological replications (8–10 leaves per replication). All experiments were repeated three times with similar results. **Indicates a significant difference according to Student's *t*-test ($P < 0.01$).

(Figure 4F). Furthermore, the presence of the leaf HR-like cell death phenotype always correlated with the upregulation of *PR* genes and the establishment of disease resistance against *Xoo* strain T1 (Figure 4G–4I); the SA level also reverted to a level consistent with the wild type in *noe2 ncs1* (Supplemental Figure 4B). Therefore, the expression of *RMC* seems to be indispensable for *noe2*-mediated HR-like cell death and activation of disease resistance.

The role of RMC in HR-like cell death

To further characterize the role of RMC in *RLS1-D*-activated leaf HR-like cell death, its expression in *noe2* plants was analyzed. In line with a previous report, *RMC* was ubiquitously expressed, with the highest expression level in the root (Figure 5A) (Jiang et al., 2007). In *noe2*, the transcript levels of *RMC* were elevated in the leaf area that exhibited the HR-like cell death phenotype compared with the non-lesion area (Figure 5B). Accordingly, the transcript level of *RMC* was increased in *RLS1-D*-overexpressing leaves with cell death (M1 and M2) and not significantly different from the wild type in the corresponding *RLS1*-repression leaves (NP^{Ri}, *noe2*^{Ri}) or *RLS1*-overexpression leaves in the *noe2* background (*noe2*-OV4 or *noe2*-OV8) (Supplemental Figure 4C). Furthermore, *RMC* expression was rapidly induced by H_2O_2 and HL treatment in 2-week-old LL-grown seedlings (Figure 5C and 5D). These results imply that the expression of *RMC* is correlated with HR-like cell death formation. Increased accumulation of RMC was also found
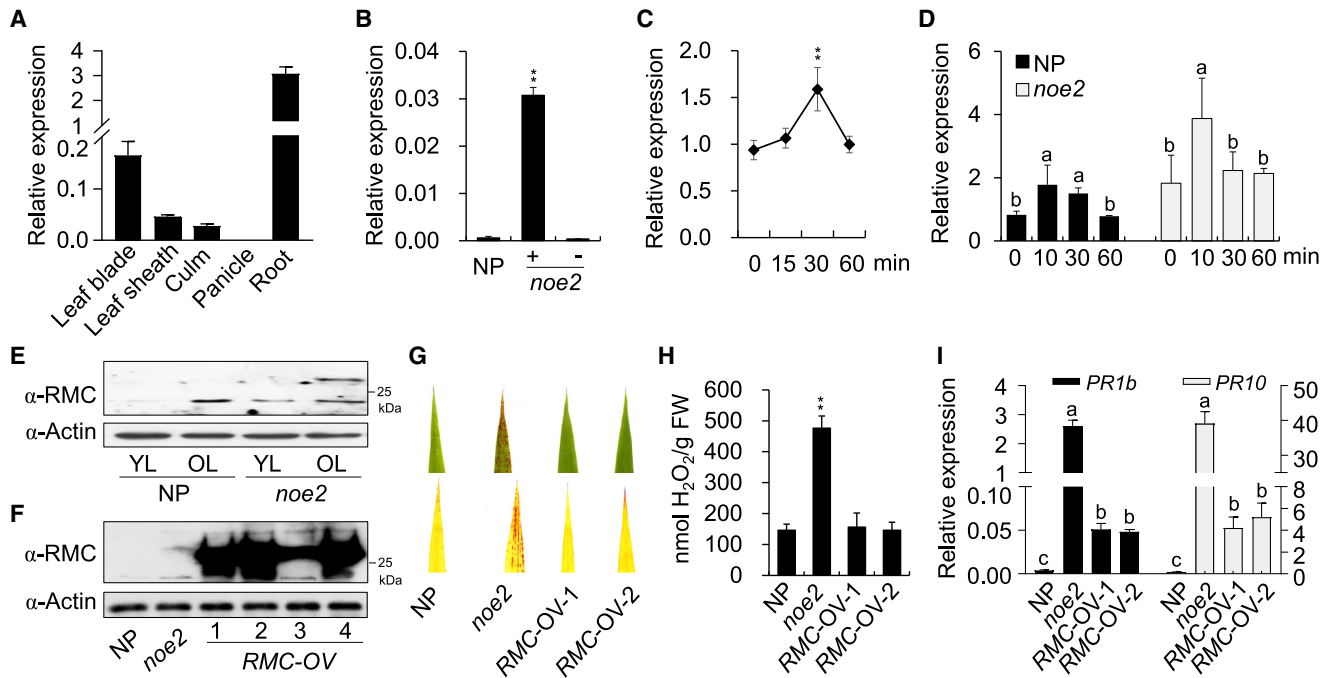
Figure 5. Expression pattern of *RMC* and evidence that over-accumulation of RMC in wild-type plants does not trigger HR-like cell death.

(A) Expression patterns of *RMC* in different tissues of rice collected at the booting stage.

(B) The expression of *RMC* in lesion ("+") and non-lesion ("−") areas of *noe2* leaves.

(C) The expression of *RMC* in 2-week-old NP seedlings in response to 50 mM H_2O_2 treatment.

(D) The expression of *RMC* in 2-week-old *noe2* seedlings in response to HL treatment (light intensity ~800 μmol m^{-2} s^{-1}) compared with the wild type.

(E) The amount of RMC protein in leaves of *noe2* and wild-type plants at the heading stage. Immunoblotting was performed with the Actin antibody as a loading control, and the level of RMC was detected by anti-RMC antibody. YL: young leaf, the first expanded leaf from top to bottom; OL: old leaf, the third leaf from top to bottom.

(F) The accumulation of RMC protein in *noe2*, wild-type, and RMC-overexpressing (*RMC*-OV) plants at the heading stage.

(G–I) H_2O_2 accumulation demonstrated by DAB staining **(G)**, H_2O_2 content **(H)**, and *PR* gene expression **(I)** of *RMC*-overexpressing lines in the wild-type background. All experiments were repeated three times with similar results. Values are the means ± SD (*n* = 3). **Indicates a significant difference according to Student's *t*-test (*P* < 0.01). Letters above bars indicate statistically different groups using a one-way ANOVA, followed by Duncan's multiple range test (*P* < 0.05).

in the leaves of the *noe2* line relative to wild-type plants. Moreover, the accumulation of RMC in leaves of wild-type and *noe2* plants increased in old leaves relative to young leaves (Figure 5E). Therefore, RMC may play a key role in both HR-like leaf cell death and leaf senescence.

To further explore whether RMC alone is sufficient to mediate the initiation of HR-like cell death, *RMC* was overexpressed in wild-type plants, and four plants with higher accumulation of RMC protein were selected (Figure 5F). None of these lines exhibited the HR-like leaf cell death phenotype or enhanced disease resistance against *Xoo* strain T1 (Figure 5G and Supplemental Figure 4D). Furthermore, the H_2O_2 content of these *RMC*-overexpressing plants was not elevated, and there was only slight induction of *PR* gene expression (Figure 5H and 5I). Therefore, overexpression of *RMC* in wild-type plants is not sufficient to trigger HR-like cell death in the presence of native RLS1.

Interaction of RLS1-D and RMC triggers HR-like cell death

To investigate a possible physical interaction between RLS1 and RMC, a yeast two-hybrid assay was employed and revealed a

physical interaction between RLS1 and RMC (Figure 6A). Interestingly, co-transformation of *RMC* and *RLS1-D* was lethal for yeast, indicating that the interaction of RMC and RLS1-D may also induce cell death even in this heterologous system (Figure 6A). A similar result was obtained from transient co-expression of *RMC* and the native *RLS1* or mutated *RLS1-D* in agro-infiltrated *Nicotiana benthamiana* leaves. Rapid leaf cell death was observed in leaves that co-expressed *RMC* and *RLS1-D* but not *RMC* and *RLS1* 2 days after infiltration (Figure 6B). However, without *RMC*, *RLS1-D* alone was unable to trigger an observable cell death phenotype on day 2 post-infiltration. Until the third day post infiltration, an observable but relatively small area of cell death appeared (Supplemental Figure 5), possibly attributable to accumulation of endogenous RMC homologs. Therefore, the presence of both RMC and RLS1-D is sufficient to initiate the HR-like cell death process.

To examine whether RMC and RLS1-D interact *in vivo*, bimolecular fluorescence complementation (BiFC) was performed. As expected, co-expression of *RMC* and *RLS1-D* triggered HR-like leaf cell death in tobacco leaves at 2 days post-infiltration; therefore, BiFC analysis was undertaken at 1 day post-infiltration before the development of HR-like cell death. Our data implied that both
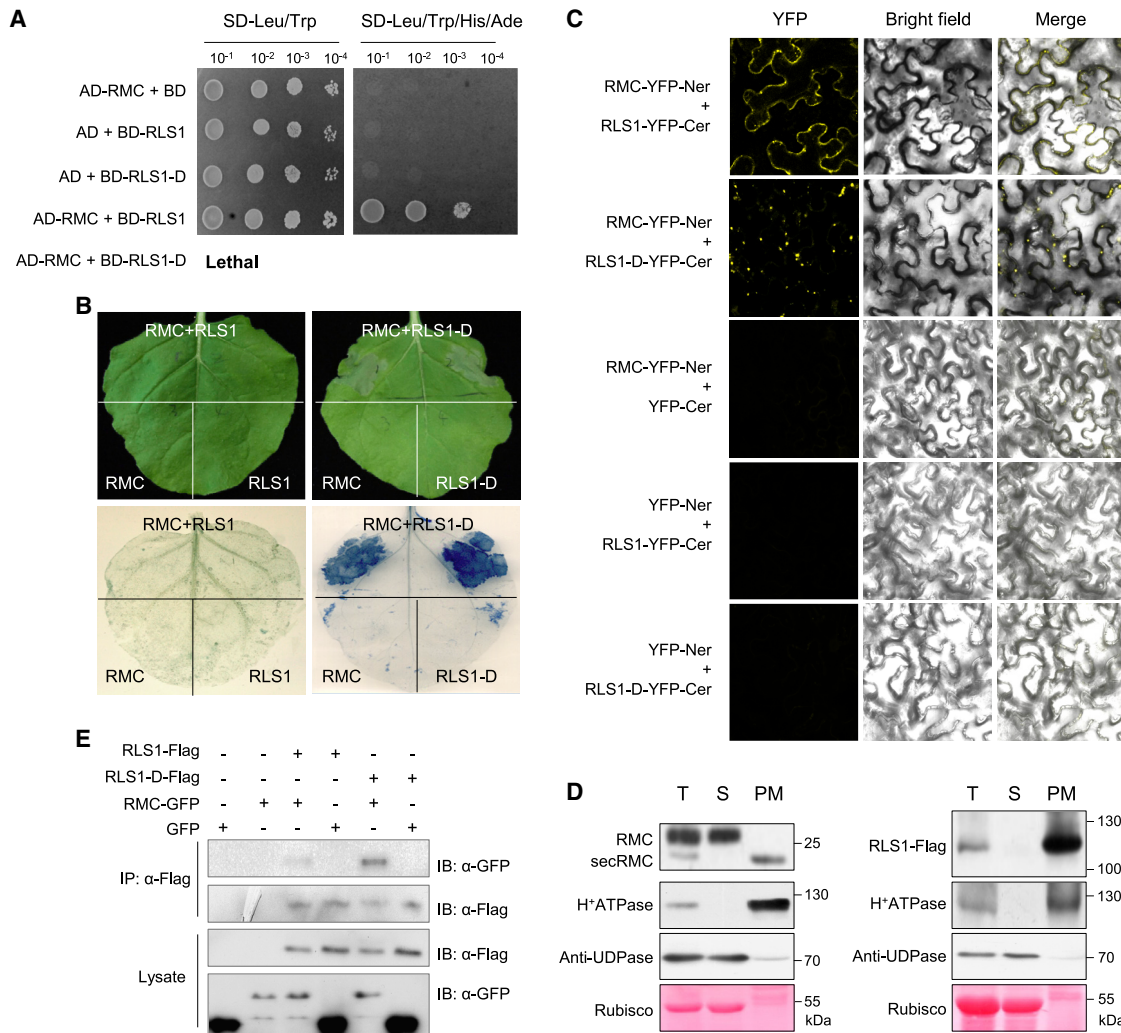
Figure 6. Co-expression of *RlS1-D* and *RMC* induced cell death and changed the pattern of subcellular localization.

(A) The co-transformation of *RLS1-D* with *RMC* was lethal in yeast, whereas co-expression of *RLS1* and *RMC* did not affect growth of yeast cells.

(B) Transient expression of *RLS1-D* together with *RMC* induced leaf cell death in *N. benthamiana* 2 days after infiltration. *Agrobacteria* containing the corresponding plasmids were infiltrated into tobacco leaves, and the results were observed at 2 days post-infiltration (dpi). Trypan blue (TB) staining shows cell death resulting from co-expression of *RLS1-D* with *RMC*.

(C) A BiFC experiment demonstrated the different interaction patterns of RLS1 and RLS1-D with RMC in the leaf of *N. benthamiana*. *Agrobacteria* containing the corresponding plasmids were infiltrated into tobacco leaves, which were observed at 1 dpi. Images were collected using a confocal laser scanning microscope (LSM 510, Zeiss, Germany).

(D) Protein fractionation experiments using leaves of *noe2* seedlings to determine the presence of RMC in total protein (T), supernatant (S), and precipitate pellets from the plasma membrane (PM). The PM protein H^+ATPase was used as a positive control to demonstrate the protein fraction derived from the PM. UDPase was used as a cytoplasm marker. Ponceau staining of the large subunit of Rubisco was used as a loading control. RMC, full-length RMC; secRMC, secreted RMC.

(E) The interaction of RMC with RLS1-D and RLS1 proteins demonstrated by co-immunoprecipitation (co-IP). Please note that the lighter band of RLS1-Flag is probably due to the greater instability of RLS1-Flag during sample preparation compared with RLS1D-Flag.

RLS1 and RLS1-D could interact with RMC (Figure 6C). Intriguingly, BiFC analysis of *RMC* and *RLS1-D* co-expression suggested that RLS1-D and RMC aggregated more extensively compared with the combination of RLS1 and RMC (Figure 6C), whereas there were no significant differences between the RLS1 and RLS1-D proteins with respect to protein localization when RMC was not co-expressed (Supplemental Figure 6). These findings indicate that the interaction of RMC and RLS1-D resulted in a change in the pattern of their subcellular localization, and this dynamic re-localization may be a feature of some NLRs during the

process of triggering HR-like cell death. Consistent with these findings, a recent study reported that a constitutively autoactive NLR in the NLR REQUIRED FOR CELL DEATH (NRC) superclade, NRC4, also showed punctate distribution that was mainly associated with the PM (Duggan et al., 2021). As a CRRSP, RMC was previously identified as a secreted protein (Zhang et al., 2009). Using RMC-GFP transgenic *Arabidopsis*, RMC was also found to localize on the PM under normal and plasmolysed conditions (Jiang et al., 2007). To clarify these findings, we used a PM extraction kit to prepare a protein fraction isolated from *noe2* seedlings, and our
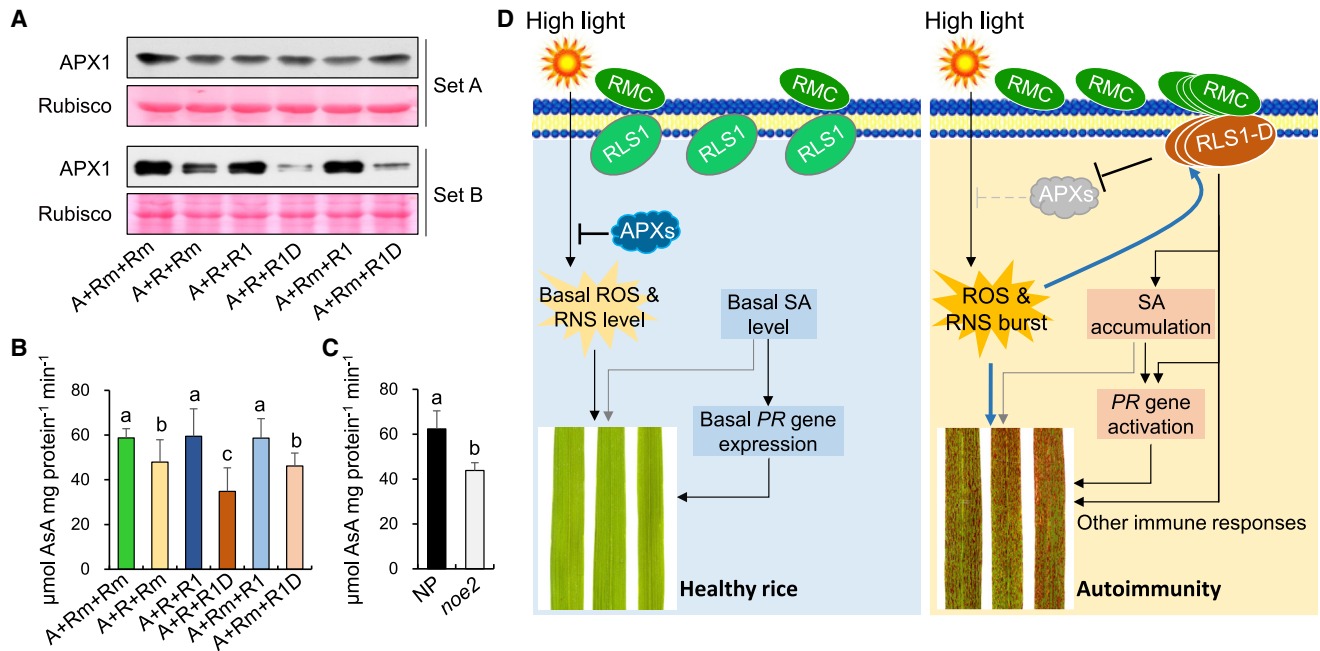
Figure 7. RLS1-D interacted with RMC to regulate the enzyme activity of APX1.

(A) Protein levels of APX1 in the indicated samples. Different *Agrobacterium* combinations of *RMC*, mutated *RMC*, *RLS1*, and *RLS1-D* were infiltrated into *APX1*-expressing tobacco leaves. Set A: within 5 min of infiltration, a group of samples were collected for western blotting, which confirmed that the initial amount of APX1 was consistent among different infiltration combinations. Set B: when the RLS1-D-induced cell death phenotype had just appeared, another group of samples were collected, and the amount of APX1 protein was detected. The level of APX1 was detected by anti-GFP antibody. A, *APX1*; R, *RMC*; Rm, mutated *RMC*; R1, *RLS1*; R1D, *RLS1-D*.

(B) *In vivo* APX enzyme activity assay using crude extracts from *N. benthamiana* leaves transiently expressing *APX1*. Co-expression of *RMC*, but not mutated *RMC*, suppressed APX1 activity. Co-expression of *RLS1-D*, but not *RLS1*, further reduced APX1 activity. Values are the means ± SD ($n = 6$).

(C) Determination of total APX enzyme activity in leaves of NP and *noe2* plants at the booting stage. Values are the means ± SD ($n = 4$). Letters above bars in **(B and C)** indicate statistically different groups using a one-way ANOVA, followed by Duncan's multiple range test ($P < 0.05$).

(D) A working model of the RLS1–RMC module in cell death development and defense responses in rice. In the wild-type plant, RLS1 remained in an auto-inhibited state, while RMC was expressed at a low level and interacted with RLS1. The ROS or RNS induced by high light during the day was scavenged promptly by the anti-oxidative system, including ascorbate peroxidases (APXs). Once RLS1 was activated as RLS-D, the RLS1-D–RMC interaction pairs aggregated in the PM and triggered defense responses, resulting in cell death accompanied by suppressed APX activity, SA accumulation, and upregulation of *PR* genes. In this process, the accumulation of ROS and RNS caused by high light and the suppression of antioxidant enzymes further induced the expression of *RMC*, which may function in a positive feedback loop to amplify the defense responses.

western blotting assays using anti-RMC antibody confirmed that RMC protein was present in both the PM and cytosol fractions (Figure 6D). Intriguingly, only secreted mature RMC protein could be detected on the PM, whereas the immature RMC protein was detected in the cytoplasm. Our western blotting assays with protein fractions also confirmed the PM localization of RLS1 (Figure 6D), confirming a spatial basis for the RMC–RLS1 interaction on the PM. The RMC–RLS1 interaction was further verified by co-immunoprecipitation experiments (Figure 6E).

Co-expression of RLS1-D and RMC triggers cell death accompanied by suppressed APX1 activity

The *noe2* mutant was identified because of its high ROS and RNS contents relative to wild-type NP plants. Our data also imply that the expression of *RLS1-D* positively affects the level of H_2O_2 (Figure 2I). In accordance with this finding, the expression levels of genes encoding antioxidant enzymes, including ascorbate peroxidases (APXs), peroxiredoxins, and catalases (CATs), were all significantly suppressed in *noe2* leaves (Supplemental Figure 7). Therefore, during RLS1-D- and RMC-activated HR-like cell death in *noe2* plants, the transcriptional in-

hibition of antioxidant enzymes further promotes ROS and RNS levels, which may accelerate the cell death process.

Interestingly, immunoprecipitation-MASS analyses using transgenic rice calli expressing RLS1-D-Flag or RMC-GFP fusion proteins identified 120 RLS1-D-interacting proteins and 255 RMC-interacting proteins, respectively. The antioxidant enzymes APX1 and CAT-B were identified as 2 of the 36 proteins that associated with both RLS1 and RMC. We therefore focused on APX1 to determine whether the activity of this antioxidant enzyme is affected at the protein level by co-expression of RLS1-D and RMC. For the APX1 enzyme activity assay, *APX1* was first transiently expressed in *N. benthamiana* leaves for 1 day. Then, different *Agrobacterium* combinations of *RMC*, *RMC* with inframe shift mutation as a negative control (*RMCm*), *RLS1*, and *RLS1-D* were infiltrated into *APX1*-expressing *N. benthamiana* leaves. Within 5 min of infiltration, a group of samples were collected for protein quantification by western blotting assays, which confirmed that the initial amount of APX1 was consistent among different infiltration combinations (Figure 7A and Supplemental Figure 8A). When the RLS1-D-induced cell death phenotype was just about to appear, another group of samples

were collected for APX1 enzyme activity assays and western blotting assays. A slight but detectable inhibitory effect of RMC on APX1 activity was observed (Figure 7B). Moreover, this assay demonstrated that RLS1-D, but not RLS1, had a significant inhibitory effect on APX1 activity, which was further strengthened by the accumulation of RMC (Figure 7B). Consistent with this observation, total APX enzyme activity was significantly decreased in the *noe2* mutant and *RMC*-overexpressing lines compared with wild-type plants (Figure 7C and Supplemental Figure 8B and 8C). All these findings revealed that, in the *noe2* mutant, the RLS1-D–RMC couple may swiftly inhibit APX1 activity to facilitate ROS accumulation, contributing to the formation of HR-like cell death. Intriguingly, this result indicated that RLS1-D–RMC may have a regulatory effect on the protein stability of APX1 *in planta* that remains to be clarified (Figure 7A). It is also worth noting that the inhibitory effect of RMC on APX1 was unexpectedly relieved by wild-type RLS1 in our assay (Figure 7B), indicating that basal expression of natural NLR proteins may play a positive role in antioxidant activity in plants.

DISCUSSION

The majority of plant R proteins belong to the NLR family, which shares a common architecture with animal NLRs, containing NBS and LRR domains. The LRR domain is implicated in auto-inhibition and/or effector detection (Jones and Jones, 1997; Qi et al., 2012), and truncated NLRs without LRRs, such as TIR-NBS protein CHS1 and TIR-NBS2, were also found to be required for activated defense responses in *Arabidopsis* (Meyers et al., 2002; Wang et al., 2013b; Zbierzak et al., 2013; Zhao et al., 2015). Structural analysis of RLS1 indicated that it had conserved NB-ARC and CC domains but with an ARM domain instead of an LRR domain at its C terminus. Therefore, RLS1 belongs to a special subfamily of plant NB-ARC proteins that differ from typical NLRs. Our data indicated that RLS1 participates in HR-like cell death and also disease resistance, revealing an immune function for this CC-NBS protein that lacks an LRR.

ARM-motif containing proteins form a large family with diverse and fundamental functions in many eukaryotes (Tewari et al., 2010). Functional analyses of plant ARM-motif-containing proteins in immunity have mainly focused on reports of plant unique U-box (PUB) E3 ubiquitin ligases in *Arabidopsis*, rice, and *N. benthamiana* (Samuel et al., 2006; Yee and Goring, 2009; Wang et al., 2015; Zhou et al., 2015; Furlan et al., 2017; Orosa et al., 2017; Trujillo, 2018). Besides PUB proteins, the rice blast resistance gene *Ptr*, which contains four ARM repeats, is reported to be required for broad-spectrum disease resistance (Zhao et al., 2018). Here, RLS1 represents another new example of ARM-containing proteins that are associated with both cell death and disease resistance. Furthermore, the HR-like cell death activated by RLS1-D is independent of NPR1 and RAR1, as the absence of NPR1 and RAR1 function in the *noe2 npr1* and *noe2 rar1* double mutants did not compromise *noe2*-mediated HR-like cell death and disease resistance (Figure 3F–3J). Thus, it appears that RLS1-D may function through a previously uncharacterized disease resistance signaling pathway.

NLR activation of ETI signaling results in massive cellular reprogramming to execute a plethora of defense responses, which are also under tight regulatory control (Elmore et al., 2011; Johnson et al., 2012). A number of proteins have been proposed to interact with NLRs, including Heat Shock Protein 90 kDa (HSP90), RAR1, Suppressor of the G2 allele of *skp1* (SGT1), Suppressor of *rps4-RLD1* (SRFR1), and Compromised recognition of TCV1 (CRT1), which are thought to be components of a complex required for NLR folding, accumulation, and regulation (Hubert et al., 2009; Zhang et al., 2010; Elmore et al., 2011). Recently, it has been suggested that interactions between NLRs and their specific guardee or decoy proteins are required for inhibition of HR. In this context, disruption of the NLR guardee protein RIN4 can induce inappropriate HR activation. Two key enzymes integral to lignin biosynthesis have also been shown to suppress HR formation by forming a complex with the NLR Rp1 (Wang et al., 2016; Balint-Kurti, 2019; Toruno et al., 2019). In contrast to these findings, our data establish that an NB-ARC–CRRSP couple is involved in the development of HR-like cell death and associated disease resistance. In this context, the CRRSP (RMC) may function as a helper of the NLR (RLS1).

It is well established that light has a significant impact on plant immunity (Hua, 2013); however, the detailed molecular mechanisms remain elusive. Our findings showed that activated RLS1 triggered HR-like cell death in an HL-dependent manner, as no lesions were found in shielded leaf areas and in seedlings grown under LL (Figure 1D–1F). *RMC* is rapidly induced at the transcriptional level within minutes by HL treatment. Moreover, it has significantly higher expression in leaf areas with lesions (Figure 5B). Recent findings have revealed the important role of JA in the acclimation of plants to a combination of HL and heat stress (Balfagon et al., 2019). Notably, we revealed that the JA content of *noe2* plants (26.07 ± 1.37 ng/g fresh weight) was about 2.3 times that of the wild-type control (11.35 ± 0.26 ng/g fresh weight). As RMC was reported to be induced by JA and subsequently integral to JA signaling (Jiang et al., 2007), JA may have a potential role in *noe2*-triggered cell death. Although further studies are required to clarify whether HL regulates the expression of *RMC* through JA signaling in leaves, our findings imply that RMC may function as a link between HL and plant immunity associated with NB-ARC protein-related activity.

In addition to induction by HL, *RMC* is also rapidly induced by H_2O_2 (Figure 5C and 5D), which may indicate the existence of a positive feedback loop (Figure 7D). That is, the accumulation of ROS and RNS resulting from HL and the associated downregulation of antioxidant systems may further induce *RMC* expression, resulting in amplification of cell death and associated immune responses (Supplemental Figure 7). Although our data support the point that the RLS1-D–RMC couple suppresses APX1 enzyme activity (Figure 7B and 7C), the mechanism(s) associated with the downregulation of expression of other antioxidant enzymes remains to be established.

Collectively, our findings identify an NB-ARC signaling partner and reveal an NB-ARC–CRRSP signaling module that modulates the development of HR-like cell death and associated disease resistance by suppression of some antioxidant defense systems (Figure 7D). It will now be important to establish whether RLS1 function is specific for RMC or whether this CRRSP is required by other NB-ARC containing proteins, i.e., NLRs for HR development and the establishment of disease resistance.

Furthermore, are there other NB-ARC/NLR–CRRSP modules associated with immunity and cell death development or perhaps other areas of plant biology? Determining whether NB-ARC–CRRSP signaling modules are restricted to rice or whether they function across plant species will also be informative. Finally, insights into the molecular mechanisms underpinning the activity of NB-ARC/NLR–CRRSP function may provide new strategies for plant breeding or rational crop design.

METHODS

Plant materials and growth conditions

Rice plants were cultivated in the experimental field of the Institute of Genetics and Developmental Biology (IGDB), Chinese Academy of Sciences (CAS), Beijing. For seedling growth and hormone treatment analyses, wild-type, mutant, and transgenic plants were hydroponically cultured with normal half-strength modified Hoagland medium for 10 days after sowing in a greenhouse with a 30°C 14 h light/24°C 10 h dark cycle. The 2-week-old seedlings were immersed for 2 h in nutrient solutions containing sodium nitroprusside (10, 25, and 50 mM) or H_2O_2 (50 mM). Twenty plants were collected for RNA isolation. All experiments were independently repeated three times.

Saville-Griess assay

To measure SNO content, the Saville-Griess assay was performed as described previously (Feechan et al., 2005; Wang et al., 2009).

Map-based cloning of *NOE2*

To map the *NOE2* gene, an F_2 population derived from a cross between *noe2* (*japonica*) and Minghui 63 (*indica*) was constructed. Genomic DNA was extracted from 306 F_2 progenies with the HR-like leaf cell death phenotype. To fine map *NOE2*, a series of polymorphic insertion-deletion markers were generated based on the different sequences between *japonica* and *indica*. The locus was finally defined to a 172-kb region, and all 29 candidate genes in this region were sequenced and analyzed using SeqMan in Lasergene version 5.0 software (DNASTAR). Primers used are listed in Supplemental Table 1.

Phylogenetic analysis

Protein sequences showing similarity to RLS1 were retrieved using public BLAST at the National Center for Biotechnology Information website (http://www.ncbi.nlm.nih.gov/). The structural relationships were calculated using ClustalW (Larkin et al., 2007), and a neighbor-joining phylogenetic tree was generated using MEGA 4.0 (Tamura et al., 2007). The professional programs of pfam (http://pfam.xfam.org/) and COILS (Lupas et al., 1991) were used to predict the CC region in RLS1.

Vector construction and plant transformation

For *RLS1/RMC* overexpression, the cDNA sequences of *RLS1/RLS1-D* and *RMC* were inserted into the *Bam*HI/*Sal*I sites of pCambia-2300-*35S* to generate the final constructs. For *NahG* overexpression, the pCambia-2300-*35S-NahG* construct was generated in a previous study (Tang et al., 2011). To make the *RLS1* RNAi construct, a 274-bp gene-specific fragment from 457 to 730 bp of the *RLS1* open reading frame was cloned into the *Bam*HI/*Xho*I sites of pCambia-2300-*35S*. To make the *RMC* and *NPR1* knockout constructs, we used the Biogle CRISPR-Cas9 vector construction kit according to the manufacturer's instructions (Biogle, China). The *noe2 rar1* double mutants were generated by crossing the *noe2* mutant with *RAR1* stable RNAi lines generated in a previous study (Tang et al., 2019). All constructs were introduced into *Agrobacterium tumefaciens* strain AGL-1. Wild-type or mutant calli were then transformed using the *Agrobacterium*-mediated method as described previously (Li et al., 2021).

For transient expression of native and mutated *RLS1*, *RMC*, and *APX1* in *N. benthamiana* leaves, the coding sequences of *RLS1/RLS1-D*, *RMC/RMCm*, and *APX1* were cloned into the *Sal*I site of pCambia-2300-*Actin1* tagged with Flag and eGFP, respectively. *Agrobacterium* GV3101 strains carrying different constructs as well as the *p19* construct were co-infiltrated into *N. benthamiana* leaves as described in a previous report (Xu, 2020). The primers used are listed in Supplemental Table 1.

Quantitative real-time PCR

Total RNA was prepared as described previously (Li et al., 2021). Quantitative real-time PCR (qRT–PCR) was performed using a Chromo4 real-time PCR detection system according to the manufacturer's instructions (Bio-Rad). Rice *OsActin1* was used as an internal control. The values reported are the means ± SD of three biological repeats. The primers used for qRT–PCR are listed in Supplemental Table 1.

Subcellular localization of RLS1 and RLS1-D

To determine the subcellular localization of RLS1 and RLS1-D in plant cells, full-length *RLS1* and *RLS1-D* coding sequences were amplified with the primers listed in Supplemental Table 1 and inserted into the *Xho*I and *Bam*HI sites of the CaMV *35S::eGFP* vector to generate CaMV *35S::RLS1-eGFP* and CaMV *35S::RLS1-D-eGFP* vectors, respectively. The binary vectors were subsequently transformed into *A. tumefaciens* GV3101. Transient expression of these constructs in *N. benthamiana* leaves was performed using the *A. tumefaciens*-mediated infiltration method (An et al., 2017). After 24 h incubation in the dark, images of the *N. benthamiana* leaves expressing GFP were obtained using a confocal laser scanning microscope (LSM 510, Zeiss, Germany).

HL treatment, histochemical staining, and H_2O_2 measurements

For the HL treatment experiment, a group of 2-week-old wild-type and mutant seedlings growing in LL were continuously exposed to HL with a light intensity of approximately 800 μmol m^{-2} s^{-1} for 6 h. This light intensity was achieved using a high-pressure 400 W sodium vapor lamp (Osram Plantastar, Germany).

For histochemical detection of H_2O_2 and cell death, 3,3′-diaminobenzidine staining and trypan blue staining were performed, respectively, as described previously (Lin et al., 2012).

Quantitative H_2O_2 measurement was performed using a hydrogen peroxide assay kit (Beyotime Biotechnology, China).

Evaluation of resistance to bacterial blight

Evaluation of disease resistance to bacterial blight was conducted according to a previous report (Tang et al., 2011). In brief, at the booting stage, rice plants grown in natural field conditions were inoculated with *Xoo* strain T7174 race 1 (T1) using the scissors-dip method (Kauffman et al., 1973). Lesion development was scored 14 days after inoculation by measuring lesion length.

Measurement of SA

About 0.2 g (fresh weight) of leaf tissue was fully ground into a powder in liquid nitrogen, weighed, and delivered to the plant hormone platform at IGDB, CAS for quantitative SA measurements using high-performance liquid chromatography or high-performance liquid chromatography–mass spectrometry (Bowling et al., 1994).

Suppressor screening and cloning of *NCS1*

The *ncs1* mutant was isolated from an M$_2$ population of the *noe2* mutant mutagenized with ethyl methanesulfonate. To clone the *NCS1* gene, an F$_2$ population derived from a cross between *noe2 ncs1* and Minghui 63 was constructed. F$_2$ progenies without *noe2*-caused lesions on older leaves were sampled to detect the genotype of *RLS1-D* with the dCAPS marker CM1. Then, 517 individuals with the *noe2* mutation in a homozygous state were collected for fine-mapping of the *NCS1* gene. The location of *NCS1*

was narrowed to a 37-kb region between the 4-33.61M and 4-33.64M markers. Genome sequencing of all six candidate genes in this region revealed a 26-bp deletion in the promoter of *LOC_Os04g56430*. Primer sequences are listed in Supplemental Table 1.

Yeast assay

The coding sequences of *RLS1/RLS1-D* and *RMC* were cloned into the yeast vectors pGBKT7 and pGADT7, respectively. The co-transformation of related AD/BD constructs was carried out using the Matchmaker Gold Yeast Two-Hybrid system (Clontech, USA) according to the manufacturer's protocol. Each yeast liquid culture originating from a co-transformed clone was serially diluted to $OD_{600} \sim 0.6$, and 2 μl dilution was inoculated onto plates containing SD/-Leu/-Trp (double dropout) negative synthetic dropout medium.

BiFC assay

The bimolecular fluorescence complementation assay in *N. benthamiana* leaves was carried out as described previously (Kang et al., 2017). *RMC*, *RLS1*, and *RLS1-D* cDNA fragments were amplified and cloned into split-YFP vectors with non-overlapping coding regions of *35S:VYNER* and *35S::VYCER*. The constructs were transformed into *Agrobacterium*. Equal volumes of *Agrobacterium* culture carrying the *-pVYNER* and *-pVYCER* constructs were infiltrated into 4-week-old *N. benthamiana* leaves. Plants were watered and cultured at 22°C in the dark for 1 day. Images were collected using a confocal laser scanning microscope (LSM 510, Zeiss, Germany). Composite figures were prepared using Zeiss LSM Image Browser software.

Cell death assay in *N. benthamiana*

Before infiltration with *Agrobacterium*, *N. benthamiana* was grown in the dark for 2 days. Then the CaMV *35S::RMC* or pCAMBIA2300-35S empty vector was first transiently expressed in *N. benthamiana* leaves for 1 day. Later, 0.2 OD *Agrobacterium* containing RLS1 or RLS1-D was infiltrated into *RMC*-expressing or non-*RMC*-expressing *N. benthamiana* leaves. Images of the *N. benthamiana* leaves were obtained using a camera after 2- and 3-day infiltration in the dark.

Cell fractionation

Fresh rice leaves (about 400 mg) were collected, and the homogenization step was performed outside of the filter using a mortar; fractions were then extracted according to the manual for the PM extraction kit (SM-005-P; Invent Biotechnologies). Using the same method, tobacco leaves expressing RLS1-FLAG were also separated into membrane and soluble protein fractions. Anti-UDPase (AS05086: cytosol; Agrisera) and anti-H$^+$-ATPase (AS07260: PM; Agrisera) antibodies were used to detect the markers indicating the cytosol and PM fractions, respectively.

Co-immunoprecipitation and immunoprecipitation-MASS

For transient expression of *RLS1-Flag*, *RLS1-D-Flag*, and *RMC-GFP* in *N. benthamiana* leaves, the coding sequences of native and mutated *RLS1* and *RMC* were cloned into the *Sal*I site of the pCambia-2300-*Actin1*-Flag and pCambia-2300-*Actin1*-eGFP vectors to create fusion constructs. *Agrobacterium* GV3101 strains carrying different construct combinations as well as the *p19* construct were co-infiltrated into *N. benthamiana* leaves. The infiltrated parts of *N. benthamiana* leaves were harvested, and the leaf tissue was ground in liquid nitrogen and re-suspended in extraction buffer (50 mM Tris–HCl [pH 7.5], 150 mM NaCl, 0.1% Triton X-100, 0.2% Nonidet P-40, 0.6 mM PMSF, 20 mM MG132, and Roche protease inhibitor mixture). The total extracts were incubated on ice for 20 min and centrifuged at 12 000 rpm for 15 min at 4°C to obtain the crude total protein. The anti-FLAG (R) M2 magnetic beads were prepared according to the manufacturer's instructions (Sigma). Approximately 0.4 ml of crude total protein from each sample was added to the beads and incubated for 4 h at 4°C with gentle rocking. The precipitated samples were washed at least four times using protein extraction buffer, and bound proteins were eluted by heating the beads in extraction

buffer at 55°C for 3 min. The eluted protein was detected by western blotting with standard protocols using anti-Flag and anti-GFP antibodies. Similarly, rice calli expressing RLS1-D-Flag or RMC-GFP fusion proteins were analyzed by immunoprecipitation with anti-Flag or anti-GFP beads, and the corresponding eluted proteins were identified by LC-MASS analysis according to a method described previously (Lin et al., 2012).

APX1 enzyme activity assay

APX1 activity was measured spectrophotometrically according to a previous report with a simple modification (Nakano and Asada, 1987; Jiang et al., 2016). In brief, a reaction mixture containing 275 μl buffer (KH_2PO_4/K_2HPO_4 [pH 7.0]), 10 μl 20 mM AsA, and 10 μl APX1 protein sample was added to a 96-well plate, and 5 μl 0.2 M H_2O_2 was added to start the reaction. The oxidation of AsA was recorded as a decrease in A_{290} using a TECAN Infinite F200/M200 plate reader (TECAN, Switzerland) at 25°C. The reaction rates were linear for at least 3 min and were corrected for AsA auto-oxidation in the presence of H_2O_2. The APX activity was calculated using an extinction coefficient of 2.8 mM^{-1} cm^{-1} for AsA, and the enzyme activity unit was defined as μmol AsA mg protein^{-1} min^{-1}.

AUTHOR CONTRIBUTIONS

Y.W., J.T., and C.C. conceived and designed the experiments. Y.W., J.T., H.L., Z.T., W.W., F.X., K.S., J.C., and Y.Q. performed the experiments. Y.W., J.T., H.L., and C.C. analyzed the data. Y.W., J.T., G.J.L., and C.C. composed the manuscript.

REFERENCES

Acharya, B.R., Raina, S., Maqbool, S.B., Jagadeeswaran, G., Mosher, S.L., Appel, H.M., Schultz, J.C., Klessig, D.F., and Raina, R. (2007). Overexpression of *CRK13*, an *Arabidopsis* cysteine-rich receptor-like kinase, results in enhanced resistance to *Pseudomonas syringae*. Plant J. **50**:488–499.

An, C., Li, L., Zhai, Q., You, Y., Deng, L., Wu, F., Chen, R., Jiang, H., Wang, H., Chen, Q., et al. (2017). Mediator subunit MED25 links the jasmonate receptor to transcriptionally active chromatin. Proc. Natl. Acad. Sci. USA **114**:E8930–E8939.

Astier, J., Rasul, S., Koen, E., Manzoor, H., Besson-Bard, A., Lamotte, O., Jeandroz, S., Durner, J., Lindermayr, C., and Wendehenne, D. (2011). S-nitrosylation: an emerging post-translational protein modification in plants. Plant Sci. **181**:527–533.

Balfagón, D., Sengupta, S., Gómez-Cadenas, A., Fritschi, F.B., Azad, R.K., Mittler, R., and Zandalinas, S.I. (2019). Jasmonic acid is required for plant acclimation to a combination of high light and heat stress. Plant Physiol. **181**:1668–1682.

Balint-Kurti, P. (2019). The plant hypersensitive response: concepts, control and consequences. Mol. Plant Pathol. **20**:1163–1178.

Bowling, S.A., Guo, A., Cao, H., Gordon, A.S., Klessig, D.F., and Dong, X. (1994). A mutation in Arabidopsis that leads to constitutive expression of systemic acquired resistance. Plant Cell **6**:1845–1857.

Caverzan, A., Bonifacio, A., Carvalho, F.E.L., Andrade, C.M.B., Passaia, G., Schünemann, M., Maraschin, F.D.S., Martins, M.O., Teixeira, F.K., Rauber, R., et al. (2014). The knockdown of chloroplastic ascorbate peroxidases reveals its regulatory role in the photosynthesis and protection under photo-oxidative stress in rice. Plant Sci. **214**:74–87.

Chen, K., Du, L., and Chen, Z. (2003). Sensitization of defense responses and activation of programmed cell death by a pathogen-induced receptor-like protein kinase in *Arabidopsis*. Plant Mol. Biol. **53**:61–74.

Chen, K., Fan, B., Du, L., and Chen, Z. (2004). Activation of hypersensitive cell death by pathogen-induced receptor-like protein kinases from Arabidopsis. Plant Mol. Biol. **56**:271–283.

Chern, M., Xu, Q., Bart, R.S., Bai, W., Ruan, D., Sze-To, W.H., Canlas, P.E., Jain, R., Chen, X., and Ronald, P.C. (2016). A genetic screen identifies a requirement for cysteine-rich-receptor-like kinases in rice NH1 (OsNPR1)-mediated immunity. PLoS Genet. **12**:e1006049.

Chisholm, S.T., Coaker, G., Day, B., and Staskawicz, B.J. (2006). Host-microbe interactions: shaping the evolution of the plant immune response. Cell **124**:803–814.

da Cunha, L., Sreerekha, M.V., and Mackey, D. (2007). Defense suppression by virulence effectors of bacterial phytopathogens. Curr. Opin. Plant Biol. **10**:349–357.

Delledonne, M., Xia, Y., Dixon, R.A., and Lamb, C. (1998). Nitric oxide functions as a signal in plant disease resistance. Nature **394**:585–588.

Delledonne, M., Zeier, J., Marocco, A., and Lamb, C. (2001). Signal interactions between nitric oxide and reactive oxygen intermediates in the plant hypersensitive disease resistance response. Proc. Natl. Acad. Sci. USA **98**:13454–13459.

Dong, X. (2004). NPR1, all things considered. Curr. Opin. Plant Biol. **7**:547–552.

Duggan, C., Moratto, E., Savage, Z., Hamilton, E., Adachi, H., Wu, C.H., Leary, A.Y., Tumtas, Y., Rothery, S.M., Maqbool, A., et al. (2021). Dynamic localization of a helper NLR at the plant-pathogen interface underpins pathogen recognition. Proc. Natl. Acad. Sci. USA **118**. e2104997118.

Durrant, W.E., and Dong, X. (2004). Systemic acquired resistance. Annu. Rev. Phytopathol. **42**:185–209.

Elmore, J.M., Lin, Z.J.D., and Coaker, G. (2011). Plant NB-LRR signaling: upstreams and downstreams. Curr. Opin. Plant Biol. **14**:365–371.

Feechan, A., Kwon, E., Yun, B.W., Wang, Y., Pallas, J.A., and Loake, G.J. (2005). A central role for S-nitrosothiols in plant disease resistance. Proc. Natl. Acad. Sci. USA **102**:8054–8059.

Furlan, G., Nakagami, H., Eschen-Lippold, L., Jiang, X., Majovsky, P., Kowarschik, K., Hoehenwarter, W., Lee, J., and Trujillo, M. (2017). Changes in PUB22 ubiquitination modes triggered by MITOGEN-ACTIVATED PROTEIN KINASE3 dampen the immune response. Plant Cell **29**:726–745.

Gaffney, T., Friedrich, L., Vernooij, B., Negrotto, D., Nye, G., Uknes, S., Ward, E., Kessmann, H., and Ryals, J. (1993). Requirement of salicylic acid for the induction of systemic acquired resistance. Science **261**:754–756.

Gassmann, W., and Bhattacharjee, S. (2012). Effector-triggered immunity signaling: from gene-for-gene pathways to protein-protein interaction networks. Mol. Plant Microbe Interact. **25**:862–868.

Grant, J.J., and Loake, G.J. (2000). Role of reactive oxygen intermediates and cognate redox signaling in disease resistance. Plant Physiol. **124**:21–29.

Greenberg, J.T., and Yao, N. (2004). The role and regulation of programmed cell death in plant-pathogen interactions. Cell Microbiol. **6**:201–211.

Hamada, M., Shoguchi, E., Shinzato, C., Kawashima, T., Miller, D.J., and Satoh, N. (2013). The complex NOD-like receptor repertoire of the coral *Acropora digitifera* includes novel domain combinations. Mol. Biol. Evol. **30**:167–176.

Heck, S., Grau, T., Buchala, A., Métraux, J.P., and Nawrath, C. (2003). Genetic evidence that expression of *NahG* modifies defence pathways independent of salicylic acid biosynthesis in the *Arabidopsis-Pseudomonas syringae* pv. tomato interaction. Plant J. **36**:342–352.

Hideg, E., Kálai, T., Kós, P.B., Asada, K., and Hideg, K. (2006). Singlet oxygen in plants–its significance and possible detection with double (fluorescent and spin) indicator reagents. Photochem. Photobiol. **82**:1211–1218.

Holt, B.F., 3rd, Belkhadir, Y., and Dangl, J.L. (2005). Antagonistic control of disease resistance protein stability in the plant immune system. Science **309**:929–932.

Hua, J. (2013). Modulation of plant immunity by light, circadian rhythm, and temperature. Curr. Opin. Plant Biol. **16**:406–413.

Hubert, D.A., He, Y., McNulty, B.C., Tornero, P., and Dangl, J.L. (2009). Specific *Arabidopsis* HSP90.2 alleles recapitulate RAR1 cochaperone function in plant NB-LRR disease resistance protein regulation. Proc. Natl. Acad. Sci. USA **106**:9556–9563.

Igari, K., Endo, S., Hibara, K.i., Aida, M., Sakakibara, H., Kawasaki, T., and Tasaka, M. (2008). Constitutive activation of a CC-NB-LRR protein alters morphogenesis through the cytokinin pathway in *Arabidopsis*. Plant J. **55**:14–27.

Inohara, N., and Nuñez, G. (2001). The NOD: a signaling module that regulates apoptosis and host defense against pathogens. Oncogene **20**:6473–6481.

Izbiańska, K., Floryszak-Wieczorek, J., Gajewska, J., Meller, B., Kuźnicki, D., and Arasimowicz-Jelonek, M. (2018). RNA and mRNA nitration as a novel metabolic link in potato immune response to phytophthora infestans. Front. Plant Sci. **9**:672.

Jiang, G., Yin, D., Zhao, J., Chen, H., Guo, L., Zhu, L., and Zhai, W. (2016). The rice thylakoid membrane-bound ascorbate peroxidase OsAPX8 functions in tolerance to bacterial blight. Sci. Rep. **6**:26104.

Jiang, J., Li, J., Xu, Y., Han, Y., Bai, Y., Zhou, G., Lou, Y., Xu, Z., and Chong, K. (2007). RNAi knockdown of *Oryza sativa* root meander curling gene led to altered root development and coiling which were mediated by jasmonic acid signalling in rice. Plant Cell Environ. **30**:690–699.

Jiao, B.B., Wang, J.J., Zhu, X.D., Zeng, L.J., Li, Q., and He, Z.H. (2012). A novel protein RLS1 with NB-ARM domains is involved in chloroplast degradation during leaf senescence in rice. Mol. Plant **5**:205–217.

Johnson, K.C.M., Dong, O.X., Huang, Y., and Li, X. (2012). A rolling stone gathers no moss, but resistant plants must gather their moses. Cold Spring Harb. Symp. Quant. Biol. **77**:259–268.

Jones, D.A., and Jones, J.D.G. (1997). The role of leucine-rich repeat proteins in plant defences. Adv. Bot. Res. **24**:89–167.

Kang, J., Li, J., Gao, S., Tian, C., and Zha, X. (2017). Overexpression of the leucine-rich receptor-like kinase gene LRK2 increases drought tolerance and tiller number in rice. Plant Biotechnol. J. **15**:1175–1185.

Kauffman, H.E., Reddy, A.P.K., Hsieh, S.P.V., and Marca, S.D. (1973). An improved technique for evaluation of resistance of rice varieties to *Xanthomonas oryzae*. Plant Dis. Rep. **57**:537–541.

Kimura, S., Hunter, K., Vaahtera, L., Tran, H.C., Citterico, M., Vaattovaara, A., Rokka, A., Stolze, S.C., Harzen, A., Meißner, L., et al. (2020). CRK2 and C-terminal phosphorylation of NADPH oxidase RBOHD regulate reactive oxygen species production in *Arabidopsis*. Plant Cell **32**:1063–1080.

Kliebenstein, D.J., Dietrich, R.A., Martin, A.C., Last, R.L., and Dangl, J.L. (1999). LSD1 regulates salicylic acid induction of copper zinc superoxide dismutase in *Arabidopsis thaliana*. Mol. Plant Microbe Interact. **12**:1022–1026.

La Camera, S., Geoffroy, P., Samaha, H., Ndiaye, A., Rahim, G., Legrand, M., and Heitz, T. (2005). A pathogen-inducible patatin-like lipid acyl hydrolase facilitates fungal and bacterial host colonization in *Arabidopsis*. Plant J. **44**:810–825.

Larkin, M.A., Blackshields, G., Brown, N.P., Chenna, R., McGettigan, P.A., McWilliam, H., Valentin, F., Wallace, I.M., Wilm, A., Lopez, R., et al. (2007). Clustal W and clustal X version 2.0. Bioinformatics **23**:2947–2948.

Lee, D.S., Kim, Y.C., Kwon, S.J., Ryu, C.M., and Park, O.K. (2017). The *Arabidopsis* cysteine-rich receptor-like kinase CRK36 regulates immunity through interaction with the cytoplasmic kinase BIK1. Front. Plant Sci. **8**:1856.

Li, Q., Xu, F., Chen, Z., Teng, Z., Sun, K., Li, X., Yu, J., Zhang, G., Liang, Y., Huang, X., et al. (2021). Synergistic interplay of ABA and BR signal in regulating plant growth and adaptation. Nat. Plants **7**:1108–1118.

Lin, A., Wang, Y., Tang, J., Xue, P., Li, C., Liu, L., Hu, B., Yang, F., Loake, G.J., and Chu, C. (2012). Nitric oxide and protein S-nitrosylation are integral to hydrogen peroxide-induced leaf cell death in rice. Plant Physiol. **158**:451–464.

Lindermayr, C. (2018). Crosstalk between reactive oxygen species and nitric oxide in plants: key role of S-nitrosoglutathione reductase. Free Radic. Biol. Med. **122**:110–115.

Lindermayr, C., and Durner, J. (2015). Interplay of reactive oxygen species and nitric oxide: nitric oxide coordinates reactive oxygen species homeostasis. Plant Physiol. **167**:1209–1210.

Lupas, A., Van Dyke, M., and Stock, J. (1991). Predicting coiled coils from protein sequences. Sciences **252**:1162–1164.

Lv, Q., Han, S., Wang, L., Xia, J., Li, P., Hu, R., Wang, J., Gao, L., Chen, Y., Wang, Y., et al. (2022). TEB/POLQ plays dual roles in protecting Arabidopsis from NO-induced DNA damage. Nucleic Acids Res. **50**:6820–6836.

Ma, L.S., Wang, L., Trippel, C., Mendoza-Mendoza, A., Ullmann, S., Moretti, M., Carsten, A., Kahnt, J., Reissmann, S., Zechmann, B., et al. (2018). The *Ustilago maydis* repetitive effector Rsp3 blocks the antifungal activity of mannose-binding maize proteins. Nat. Commun. **9**:1711.

Mantelin, S., Peng, H.C., Li, B., Atamian, H.S., Takken, F.L.W., and Kaloshian, I. (2011). The receptor-like kinase SlSERK1 is required for Mi-1-mediated resistance to potato aphids in tomato. Plant J. **67**:459–471.

Meyers, B.C., Morgante, M., and Michelmore, R.W. (2002). TIR-X and TIR-NBS proteins two new families related to disease resistance TIR-NBS-LRR proteins encoded in Arabidopsis and other plant genomes. Plant J. **32**:77–92.

Miyakawa, T., Miyazono, K.i., Sawano, Y., Hatano, K.i., and Tanokura, M. (2009). Crystal structure of ginkbilobin-2 with homology to the extracellular domain of plant cysteine-rich receptor-like kinases. Proteins **77**:247–251.

Nakano, Y., and Asada, K. (1987). Purification of ascorbate peroxidase in spinach-chloroplasts - its inactivation in ascorbate-depleted medium and reactivation by monodehydroascorbate radical. Plant Cell Physiol. **28**:131.

Noutoshi, Y., Ito, T., Seki, M., Nakashita, H., Yoshida, S., Marco, Y., Shirasu, K., and Shinozaki, K. (2005). A single amino acid insertion in the WRKY domain of the *Arabidopsis* TIR-NBS-LRR-WRKY-type disease resistance protein SLH1 (sensitive to low humidity 1) causes activation of defense responses and hypersensitive cell death. Plant J. **43**:873–888.

Orosa, B., He, Q., Mesmar, J., Gilroy, E.M., McLellan, H., Yang, C., Craig, A., Bailey, M., Zhang, C., Moore, J.D., et al. (2017). BTB-BACK domain protein POB1 suppresses immune cell death by targeting ubiquitin E3 ligase PUB17 for degradation. PLoS Genet. **13**:e1006540.

Qi, D., DeYoung, B.J., and Innes, R.W. (2012). Structure-function analysis of the coiled-coil and leucine-rich repeat domains of the RPS5 disease resistance protein. Plant Physiol. **158**:1819–1832.

Samuel, M.A., Salt, J.N., Shiu, S.H., and Goring, D.R. (2006). Multifunctional arm repeat domains in plants. Int. Rev. Cytol. **253**:1–26.

Serra, T.S., Figueiredo, D.D., Cordeiro, A.M., Almeida, D.M., Lourenço, T., Abreu, I.A., Sebastián, A., Fernandes, L., Contreras-Moreira, B., Oliveira, M.M., et al. (2013). OsRMC, a negative regulator of salt stress response in rice, is regulated by two AP2/ERF transcription factors. Plant Mol. Biol. **82**:439–455.

Shirano, Y., Kachroo, P., Shah, J., and Klessig, D.F. (2002). A gain-of-function mutation in an *Arabidopsis* toll interleukin1 receptor-nucleotide binding site-leucine-rich repeat type *R* gene triggers defense responses and results in enhanced disease resistance. Plant Cell **14**:3149–3162.

Shiu, S.H., and Bleecker, A.B. (2001). Receptor-like kinases from Arabidopsis form a monophyletic gene family related to animal receptor kinases. Proc. Natl. Acad. Sci. USA **98**:10763–10768.

Takken, F.L.W., and Tameling, W.I.L. (2009). To nibble at plant resistance proteins. Science **324**:744–746.

Tameling, W.I.L., Vossen, J.H., Albrecht, M., Lengauer, T., Berden, J.A., Haring, M.A., Cornelissen, B.J.C., and Takken, F.L.W. (2006). Mutations in the NB-ARC domain of I-2 that impair ATP hydrolysis cause autoactivation. Plant Physiol. **140**:1233–1245.

Tamura, K., Dudley, J., Nei, M., and Kumar, S. (2007). MEGA4: molecular evolutionary genetics analysis (MEGA) software version 4.0. Mol. Biol. Evol. **24**:1596–1599.

Tang, J., Wang, Y., Yin, W., Dong, G., Sun, K., Teng, Z., Wu, X., Wang, S., Qian, Y., Pan, X., et al. (2019). Mutation of a nucleotide-binding leucine-rich repeat immune receptor-type protein disrupts immunity to bacterial blight. Plant Physiol. **181**:1295–1313.

Tang, J., Zhu, X., Wang, Y., Liu, L., Xu, B., Li, F., Fang, J., and Chu, C. (2011). Semi-dominant mutations in the CC-NB-LRR-type R gene, NLS1, lead to constitutive activation of defense responses in rice. Plant J. **66**:996–1007.

Tewari, R., Bailes, E., Bunting, K.A., and Coates, J.C. (2010). Armadillo-repeat protein functions: questions for little creatures. Trends Cell Biol. **20**:470–481.

Toruño, T.Y., Shen, M., Coaker, G., and Mackey, D. (2019). Regulated disorder: posttranslational modifications control the RIN4 plant immune signaling hub. Mol. Plant Microbe Interact. **32**:56–64.

Trujillo, M. (2018). News from the PUB: plant U-box type E3 ubiquitin ligases. J. Exp. Bot. **69**:371–384.

Urbach, J.M., and Ausubel, F.M. (2017). The NBS-LRR architectures of plant R-proteins and metazoan NLRs evolved in independent events. Proc. Natl. Acad. Sci. USA **114**:1063–1068.

Vaattovaara, A., Brandt, B., Rajaraman, S., Safronov, O., Veidenberg, A., Luklová, M., Kangasjärvi, J., Löytynoja, A., Hothorn, M., Salojärvi, J., et al. (2019). Mechanistic insights into the evolution of DUF26-containing proteins in land plants. Commun. Biol. **2**:56.

van der Biezen, E.A., and Jones, J.D. (1998). The NB-ARC domain: a novel signalling motif shared by plant resistance gene products and regulators of cell death in animals. Curr. Biol. **8**:R226–R227.

Vranová, E., Inzé, D., and Van Breusegem, F. (2002). Signal transduction during oxidative stress. J. Exp. Bot. **53**:1227–1236.

Wang, J., Qu, B., Dou, S., Li, L., Yin, D., Pang, Z., Zhou, Z., Tian, M., Liu, G., Xie, Q., et al. (2015). The E3 ligase OsPUB15 interacts with the receptor-like kinase PID2 and regulates plant cell death and innate immunity. BMC Plant Biol. **15**:49.

Wang, J., Wang, Y., Liu, X., Xu, Y., and Ma, Q. (2016). Microtubule polymerization functions in hypersensitive response and accumulation of H_2O_2 in wheat induced by the stripe rust. BioMed Res. Int. **2016**:7830768.

Wang, Y., Lin, A., Loake, G.J., and Chu, C. (2013a). H_2O_2-induced leaf cell death and the crosstalk of reactive nitric/oxygen species. J. Integr. Plant Biol. **55**:202–208.

Wang, Y., Zhang, Y., Wang, Z., Zhang, X., and Yang, S. (2013b). A missense mutation in CHS1, a TIR-NB protein, induces chilling sensitivity in Arabidopsis. Plant J. **75**:553–565.

Wang, Y.Q., Feechan, A., Yun, B.W., Shafiei, R., Hofmann, A., Taylor, P., Xue, P., Yang, F.Q., Xie, Z.S., Pallas, J.A., et al. (2009). S-nitrosylation of AtSABP3 antagonizes the expression of plant immunity. J. Biol. Chem. **284**:2131–2137.

Wendehenne, D., Durner, J., and Klessig, D.F. (2004). Nitric oxide: a new player in plant signalling and defence responses. Curr. Opin. Plant Biol. **7**:449–455.

Wrzaczek, M., Brosché, M., Salojärvi, J., Kangasjärvi, S., Idänheimo, N., Mersmann, S., Robatzek, S., Karpiński, S., Karpińska, B., and Kangasjärvi, J. (2010). Transcriptional regulation of the CRK/DUF26 group of receptor-like protein kinases by ozone and plant hormones in Arabidopsis. BMC Plant Biol. **10**:95.

Xu, Y. (2020). Pull-down and co-immunoprecipitation assays of interacting proteins in plants. Chin. Bull. Bot. **1**:62–68.

Yadeta, K.A., Elmore, J.M., Creer, A.Y., Feng, B., Franco, J.Y., Rufian, J.S., He, P., Phinney, B., and Coaker, G. (2017). A cysteine-rich protein kinase associates with a membrane immune complex and the cysteine residues are required for cell death. Plant Physiol. **173**:771–787.

Yee, D., and Goring, D.R. (2009). The diversity of plant U-box E3 ubiquitin ligases: from upstream activators to downstream target substrates. J. Exp. Bot. **60**:1109–1121.

Yu, M., Lamattina, L., Spoel, S.H., and Loake, G.J. (2014). Nitric oxide function in plant biology: a redox cue in deconvolution. New Phytol. **202**:1142–1156.

Yun, B.W., Feechan, A., Yin, M., Saidi, N.B.B., Le Bihan, T., Yu, M., Moore, J.W., Kang, J.G., Kwon, E., Spoel, S.H., et al. (2011). S-nitrosylation of NADPH oxidase regulates cell death in plant immunity. Nature **478**:264–268.

Zbierzak, A.M., Porfirova, S., Griebel, T., Melzer, M., Parker, J.E., and Dörmann, P. (2013). A TIR-NBS protein encoded by Arabidopsis Chilling Sensitive 1 (CHS1) limits chloroplast damage and cell death at low temperature. Plant J. **75**:539–552.

Zhang, L., Tian, L.H., Zhao, J.F., Song, Y., Zhang, C.J., and Guo, Y. (2009). Identification of an apoplastic protein involved in the initial phase of salt stress response in rice root by two-dimensional electrophoresis. Plant Physiol. **149**:916–928.

Zhang, M., Kadota, Y., Prodromou, C., Shirasu, K., and Pearl, L.H. (2010). Structural basis for assembly of Hsp90-Sgt1-CHORD protein complexes: implications for chaperoning of NLR innate immunity receptors. Mol. Cell **39**:269–281.

Zhang, Y., Goritschnig, S., Dong, X., and Li, X. (2003). A gain-of-function mutation in a plant disease resistance gene leads to constitutive activation of downstream signal transduction pathways in *suppressor of npr1-1, constitutive 1*. Plant Cell **15**:2636–2646.

Zhao, H., Wang, X., Jia, Y., Minkenberg, B., Wheatley, M., Fan, J., Jia, M.H., Famoso, A., Edwards, J.D., Wamishe, Y., et al. (2018). The rice blast resistance gene Ptr encodes an atypical protein required for broad-spectrum disease resistance. Nat. Commun. **9**, 2039.

Zhao, T., Rui, L., Li, J., Nishimura, M.T., Vogel, J.P., Liu, N., Liu, S., Zhao, Y., Dangl, J.L., and Tang, D. (2015). A truncated NLR protein, TIR-NBS2, is required for activated defense responses in the exo70B1 mutant. PLoS Genet. **11**:e1004945.

Zhou, J., Lu, D., Xu, G., Finlayson, S.A., He, P., and Shan, L. (2015). The dominant negative ARM domain uncovers multiple functions of PUB13 in Arabidopsis immunity, flowering, and senescence. J. Exp. Bot. **66**:3353–3366.